Table 7.   Consistency of the Results Obtained by Multiplex Polymerase Chain Reaction (PCR) with those Obtained by Commercially Available Viral Examination

Patient No.	Viral examination by multiplex PCR	Viral examination by commercial laboratory test*	Results of viral serological tests*	Consistency
5	EBV (−)	EBV serological test: previous infection	VCA–IgM (−), VCA–IgG (+), EBNA IgG (+)	yes
7	CMV (−)	CMV antigenemia (−)	IgM (−), IgG (+)	yes
	EBV (−)	EBV serological test: previous infection	VCA–IgM (−), VCA–IgG (+), EBNA IgG (+)	
11	CMV (−)	CMV serological test	IgM (−), IgG (+)	yes
	EBV (−)	EBV serological test } previous infection	VCA–IgM (−), VCA–IgG (+), EA–IgG (−), EBNA IgG (+)	
	HSV (−)	HSV–1 serological test	IgM (−), IgG (+)	
18	CMV (+)	CMV serological test: reactivation/IgM antibody (+)	IgM (+), IgG (+)	yes
	EBV (−)	EBV serological test: primary infection	VCA–IgM (+), VCA–IgG (+), EA–IgG (−), EBNA–IgG (+)	no
19	EBV(+)	EBV serological test: primary infection	VCA–IgM (−), VCA–IgG (+)	no
20	CMV (+)	CMV pp65 antigenemia assay: positive	IgM (−), IgG (+)	yes
21	CMV(+)	CMV pp65 antigenemia assay: positive	IgM (+), IgG (+)	yes
		CMV serological test: reactivation/IgM antibody (+)		
	EBV(−)	EBV serological test: primary infection	VCA–IgM (+), VCA–IgG (+), EA–IgG (+−), EBNA–IgG (+)	no
29	CMV (−)	CMV serological test: previous infection	IgM (−), IgG (+)	yes
	EBV (−)	EBV serological test: previous infection	VCA–IgM (−), VCA–IgG (+), EA–IgG (+−), EBNA–IgG (+)	
37	CMV(−)	CMV serological test: previous infection	IgM (−), IgG (+)	yes
	EBV(−)	EBV serological test: previous infection	VCA–IgM (−), VCA–IgG (+), EA–IgG (+−), EBNA–IgG (+)	
	HSV–1(−)	HSV–1 serological test: previous infection	IgM (−), IgG (+),	
40	CMV(+)	colon biopsy**; immunohistochemistry: positive	IgM (−), IgG (+−)	yes
	EBV(+)	EB serological test: previous infection	VCA–IgM (−), VCA–IgG (+), EBNA–IgG (+)	no

CMV: cytomegalovirus, EBV: Epstein–Barr Virus, HSV: herpes simplex virus
*: Performed by Mitsubishi Chemical Medience Corporation, Tokyo, Japan. Positivity of serological test was determined based on positive IgM antibody.
**: Performed in our institution

Table 8. The Comparison of Hepatitis Virus PCR with Routine Method

Age	Sex	Type of hepatitis	Qualitative PCR	Quantative PCR	Commercially available PCR*
79	F	HBV	positive	1.88×10^9	7.94×10^7
69	F	HBV	positive	4.39×10^7	2.51×10^7
57	M	HBV	positive	1.49×10^8	1.25×10^8
80	M	HBV	positive	1.59×10^9	1.26×10^9
79	M	HBV	positive	1.60×10^8	7.94×10^6
63	F	HBV	positive	2.90×10^3	5.01×10^3
75	M	HBV	negative	1.00×10^1	$<3.91 \times 10^3$
63	M	HCV	N.E.	2.51×10^6	2.00×10^6
70	F	HCV	N.E.	7.94×10^4	1.00×10^5
46	M	HCV	N.E.	3.98×10^5	2.51×10^6
80	M	HCV	N.E.	2.51×10^6	1.00×10^7
66	M	HCV	N.E.	5.01×10^3	1.00×10^4
71	F	HCV	N.E.	6.31×10^5	1.26×10^6
85	F	HCV	N.E.	2.51×10^6	6.31×10^5

HBV: hepatitis B, HCV: hepatitis C, N.E.: Not examined
*: performed by Special Research Laboratory, Hachioji, Japan

sidual giant proerythroblasts. A diagnosis of PRCA due to ParvoB19 was made, and the assay for ParvoB19 showed 6.9×10^7 copies/mL in accordance with a positive qualitative PCR result and a positive serological IgM test for ParvoB19 (performed by SRL).

Discussion

The present study found a high incidence of viremia in patients with unexplained liver dysfunction and undetermined inflammation. The high proportion of hematologic malignancies including allogeneic bone marrow transplantation, that were underlying diseases in the patients included in this study may explain the high incidence of viremia. The multiplex PCR procedure appeared to be very useful in the clarification of uncertain liver dysfunction and inflammation. The patients in this cohort turned out to be highly immuno-deficient and susceptible to viral infection. The identification of the high incidence of viremia may lead to better management of these patients.

TTV (22) was the most frequently detected virus in the present study; however, the relationship between TTV-positivity and the history of transfusion was unclear as shown in Table 4, thus suggesting a previous TTV infection in these TTV-positive patients. All patients in whom TTV was detected exhibited mild to moderate hepatitis, as observed in previous reports (22), except for patients 11 and 15. The lever dysfunction improved after a short time in these 2 patients, suggesting a transient exacerbation of TTV-related liver dysfunction by immunosuppressive treatment. This possibility, however, should be elucidated in the future in a larger cohort of immune-deficient patients because the relationship between the changes of liver dysfunction and TTV load was unclear in the follow-up examination. Similar incidences of HHV-6 viremia and TTV were observed in the present study. Apart from TTV that is widely distributed in the healthy population (22, 23), HHV-6 viremia is considered to be re-activation of this virus (24); therefore, this

viremia indicates a severe immune-compromised condition. The high incidence of HHV-6 viremia in the present study could be explained by the high proportion of patients that underwent allogeneic or autologous hematopoietic stem cell transplantation or patients with hematologic malignancies, or AIDS. HHV-6 viremia occasionally advances to encephalitis or pneumonitis if its load is high (25). Therefore, identification of HHV-6 viremia is very important, and antiviral treatment is required. The present study, found that liver dysfunction was improved as the load of HHV-6 decreased in all 6 patients that were re-assayed for HHV-6 (Tables 4, 5). This suggests that liver dysfunction may be closely related to HHV-6 infection. While 2 of 17 patients in whom HHV-6 was detected showed normal liver function (Table 6), which is consistant with previous reports describing that hepatitis is not a major clinical manifestation of HHV-6 infection (26). In contrast, HHV-6-related hepatitis is reported in patients that underwent heart transplantation (27); therefore, the exact relationship between HHV-6 infection and hepatitis in immune-compromised patients should be clarified in the future. It was also important that the liver dysfunction acted as a proband that led to the discovery of serious viremia in the present study.

EBV and CMV infections can be categorized into 2 groups; primary infections that cause infectious mononucleosis (IM), and re-activation of both viruses. The present study, identified 2 patients with IM due to CMV (28) and 1 with EBV-IM (29). IM can be easily diagnosed because of its characteristic clinical picture. However, the multiplex PCR assay had definite advantages because it provided rapid results. The clinical significance of the re-activation of these 2 viruses is similar to that of HHV-6, and again in this situation, the assay system appeared to be highly useful.

There were some discrepancies regarding EBV detection between the results obtained by multiplex PCR and those obtained by routine serological tests as previously described. Patients 18 and 21, showed re-activation or primary infection patterns for both CMV and EBV when examined by routine serological methods, while EBV was not detected by the assay system. EBV-IM appeared to be atypical in these 2 patients because of the normal white cell count. Furthermore, cross-reactivity of EBV-specific IgM antibodies with CMV-antigens (30) or false positive EBV IgM serological tests (31) occasionally observed. Therefore, their IM may have been CMV-induced. EBV was detected in Patient 40, regardless of the previous infection pattern determined by the serological method. This patient had ulcerative colitis and was in an immune-deficient state. Persistent EBV viremia is likely in such conditions, and normal immune responses that produce the IgM antibody may be suppressed. Although the assay system appears to be reliable, further improvement of our system is necessary.

The authors state that they have no Conflict of Interest (COI).

References

1. Sugita S, Shimizu N, Watanabe K, et al. Use of multiplex PCR and real-time PCR to detect human herpes virus genome in ocular fluids of patients with uveitis. Br J Ophthalmol **92**: 928-932, 2008.

2. Gatto F, Cassina G, Broccolo F, et al. A multiplex calibrated real-time PCR assay for quantitation of DNA of EBV-1 and 2. J Virol Methods **78**: 98-105, 2011.

3. Burrows J, Nitsche A, Bayly B, Walker E, Higgins G, Kok T. Detection and subtyping of herpes simplex virus in clinical samples by LightCycler PCR, enzyme immunoassay and cell culture. BMC Microbiol **2**: 12, 2002, PMCID:PMC116582.

4. Espy MJ, Teo R, Ross TK, et al. Diagnosis of Varicella-Zoster virus infections in the Clinical laboratory by LightCycler PCR. J Clin Microbiol **38**: 3187-3189, 2000.

5. Schaade L, Kockelkorn P, Ritter K, Kleines M. Detection of cytomegalovirus DNA in human specimens by LightCycler PCR. J Clin Microbiol **38**: 4006-4009, 2000.

6. Ohyashiki JH, Suzuki A, Aritaki K, et al. Use of real-time PCR to monitor human herpesvirus 6 reactivation after allogeneic bone marrow transplantation. Int J Mol Med **6**: 427-432, 2000.

7. Boivin G, Côté S, Cloutier N, Abed Y, Maguigad M, Routy JP. Quantification of human herpesvirus 8 by real-time PCR in blood fractions of AIDS patients with Kaposi's sarcoma and multicentric Castleman's disease. J Med Virol **68**: 399-403, 2002.

8. Harder TC, Hufnagel M, Zahn K, et al. New LightCycler PCR for rapid and sensitive quantification of Parvovirus B19 DNA guides therapeutic decision-making in relapsing infections. J Clin Microbiol **39**: 4413-4419, 2001.

9. Whiley DM, Mackay IM, Sloots TP. Detection and differentiation of human polyomaviruses JC and BK by LigtCycler PCR. J Clin Microbiol **39**: 4357-4361, 2001.

10. Nishizawa T, Okamoto H, Konishi K, Yoshizawa H, Miyakawa Y, Mayumi M. A novel DNA virus (TTV) associated with elevated transaminase levels in posttransfusion hepatitis of unknown etiology. Biochem Biopsy Res Commun **241**: 92-97, 1997.

11. Corey L, Huang ML, Selke S, Wald A. Differentiation of herpes simplex virus types 1 and 2 in clinical samples by a real-time taqman PCR assay. J Med Viol **76**: 350-355, 2005.

12. Kimura H, Morita M, Yabuta Y, et al. Quantitative analysis of Epstein-Barr virus load by using a real-time PCR assay. J Clin Microbiol **37**: 132-136, 1999.

13. Piiparinen H, Helanterä I, Lappalainen M, et al. Quantitative PCR in the diagnosis of CMV infection and in the monitoring of viral load during the antiviral treatment in renal transplant patients. J Med Virol **76**: 367-372, 2005, PMID: 15902704.

14. Watzinger F, Suda M, Preuner S, et al. Real-time quantitative PCR assays for detection and monitoring of pathogenic human viruses in immunosuppressed pediatric patients. J Clin Microbiol **42**: 5189-5198, 2004.

15. Hara S, Kimura H, Hosino Y, et al. Detection of herpesvirus DNA in the serum of immunocompetent children. Microbiol Immunol **46**: 177-180, 2002, PMID:12008926.

16. Polstra AM, Van Den Burg R, Goudsmit J, Cornelissen M. Human herpesvirus 8 load in matched serum and plasma samples of patients with AIDS-associated Kaposi's sarcoma. J Clin Microbiol **41**: 5488-5491, 2003.

17. Herman J, Van Ranst M, Snoeck K, Beusekinck K, Lerut E, Van Damme-Lombaerts R. Polyomavirus infection in pediatric renal transplant recipients: evaluation using a quantitative real-time PCR technique. Pediatr Transplant **8**: 485-492, 2004.

18. Le Gal F, Gordien E, Affolabi D, et al. Quantification of hepatitis delta virus RNA in serum by consensus real-time PCR indicates different patterns of virological response to interferon therapy in chronically infected patients. J Clin Microbiol **43**: 2363-2369, 2005.

19. Jothikumar N, Cromeans TL, Robertson BH, Meng XJ, Hill VR. A broadly reactive one-step real-time RT-PCR assay for rapid and sensitive detection of hepatitis E virus. J Virol Methods **131**: 65-71, 2006, PMID: 16125257.

20. Künkel U, Höhne M, Berg T, et al. Quality control study on the performance of GB virus C/hepatitis G virus PCR. J Hepatol **28**: 978-984, 1998.

21. Moen EM, Sleboda J, Grinde B. Real-time PCR methods for independent quantitation of TTV and TLMV. J Viol Method **104**: 59-67, 2002.

22. Biagini P. Human circoviruses. Vet Microbiol **98**: 95-101, 2004.

23. Gallian P, Biagini P, Zhong S, et al. TT virus: a study of molecular epidemiology and transmission of genotypes 1, 2 and 3. J Clin Virol **17**: 43-49, 2000.

24. Zerr DN, Corey L, Kim HW, Huang ML, Nguy L, Borckh M. Clinical outcomes of human herpesvirus 6 reactivation after hematopoietic stem cell transplantation. Clin Infect Dis **40**: 932-940, 2005.

25. Ogata M, Satou T, Kawano R, et al. Correlations of HHV-6 viral load and plasma IL-6 concentration with HHV-6 encephalitis in allogeneic stem cell transplant recipients. Bone Marrow Transplant **45**: 129-136, 2010.

26. Zerr DM. Human herpesvirus 6: a clinical update. Herpes **13**: 20-24, 2006.

27. Robert C, Agut H, Lunel-Fabian F, Leger P. Human herpesvirus 6 infection and hepatitis following heart transplantation. Presse Med **23**: 1209-1210, 1994.

28. Han XY, Hellerstedt BA, Koller CA. Postsplenectomy cytomegalovirus mononucleosis is a distinct clinicopathologic syndrome. Am J Med Sci **339**: 395-399, 2010.

29. Vouloumanou EK, Rafailidis PI, Falagas ME. Current diagnosis and management of infectious mononucleosis. Curr Opin Hematol **19**: 14-20, 2012.

30. Lang D, Vornhagen R, Rothe M, Hinderer W, Sonneborn H-H, Plachter B. Cross-reactivity of Epstein-Barr virus-specific immunogloburin M antibodies with cytomegalovirus antigens containing glycine homopolymers. Clin Diagn Lab Immunol **8**: 747-756, 2001.

31. Just-Nübling G, Korn S, Ludwig B, Stephan C, Doerr HW, Preiser W. Primary cytomegalovirus infection in an outpatient setting: laboratory markers and clinical aspects. Infection **31**: 318-323, 2003.

Current Topics

Stem Cell Research for Regenerative Medicine/Personalized Medicine

Angiogenic Cell Therapy for Severe Ischemic Diseases

Teruhide Yamaguchi,* Toshie Kanayasu-Toyoda, and Eriko Uchida

Division of Biological Chemistry and Biologicals, National Institute of Health Sciences;
1–18–1 Kamiyoga, Setagaya-ku, Tokyo 158–8501, Japan.

Cell therapies for severe ischemic diseases such as limb ischemia, acute myocardial infarction, and cerebral ischemia have been developed through *in vitro* and *in vivo* animal and clinical studies. Active cells for angiogenic cell therapy are believed endothelial progenitor cells (EPCs). EPCs have been extensively investigated to clarify their origin and biology. Many sources of EPCs have been proposed, including mononuclear cells (MNCs) fraction containing CD34$^+$ or CD133$^+$ (AC133$^+$), isolated CD34$^+$ and AC133$^+$ cells, and induction and differentiation of EPCs from hematopoietic stem cells (HSCs). However, *in vivo* mechanisms by which EPCs contribute to neovascularization should be clarified. Many *in vitro*, *in vivo*, and clinical studies have been performed using these cells; angiogenic cell therapy will become an important regimen for severe ischemic diseases.

Key words   endothelial progenitor cell; cell therapy; angiogenesis; CD34; AC133

1. INTRODUCTION

Over the past one and a half decades, cell therapies (therapeutic angiogenesis) for ischemic disease caused by arterial infarction such as acute myocardial infarction, severe limb ischemia, Buerger disease, and cerebral infarction have been developed. First of all, the finding of endothelial progenitor cells (EPCs) in peripheral blood is a key topic for therapeutic angiogenesis.[1] EPCs were first isolated as CD34$^+$ cells in mononuclear cells (MNCs) from adult blood.[1,2] Asahara *et al.*[1] reported that putative endothelial cell (EC) progenitors or angioblasts were isolated from human peripheral blood by magnetic bead selection on the basis of cell surface antigen (CD34) expression. These cells differentiated into ECs *in vitro*. In animal models of ischemia, heterologous, homologous, and autologous EC progenitor cells incorporate into sites of active angiogenesis. They concluded that EC progenitors might be useful for augmenting collateral vessel growth to ischemic tissues.

In response to tissue ischemia, EPCs are believed mobilized from bone marrow to peripheral blood, and then migrate into specific ischemic regions such as sites of nascent neovascularization. Multiple sources of EPCs have been reported such as MNC fraction of peripheral blood, bone marrow MNCs, and granulocyte-colony stimulating factor (G-CSF)-mobilized CD34$^+$/AC133$^+$ cells.[3]

2. MONONUCLEAR CELL THERAPY FOR ANGIOGENESIS

Target diseases of cell therapy for angiogenesis vary from ischemic limb, myocardial infarction, and cerebral infarction. EPCs or stem cells for EPC are believed suitable as cell sources for the treatment of these diseases. Autologous MNCs derived from bone marrow or peripheral blood are often used to treat ischemic diseases. MNCs from peripheral blood of patients pre-treated with G-CSF are also used in angiogenesis cell therapy. Whatever resource of mononuclear cells is used, it is expected that the cells contain EPCs or stem cells for EPCs.

On the other hand, not only MNCs but also selected CD34$^+$ cells have been used for the treatment of ischemic diseases. While CD34 is a general marker of hematopoietic stem cells (HSC), EPCs also express CD34 antigen and are differentiated from CD34$^+$ cells derived from either bone marrow or peripheral blood cells. Since it seems not feasible efficiently to purify EPCs from MNC fraction or whole blood, many clinical studies using MNCs containing CD34$^+$ cells have been conducted. Asahara *et al.* reported that chemically labeled CD34$^+$ cells integrated into new capillaries that selectively form into ischemic leg using murine model of limb ischemia, suggesting that injected CD34$^+$ cells integrated into vascularization.

2.1. Cell Therapy for Limb Ischemia Matoba *et al.*[4] attempted angiogenic cell therapy by intramuscular injection of autologous bone marrow MNCs (BM-MNCs) in patients with peripheral artery disease (PAD) and critical limb ischemia. Feasibility was shown by the randomized controlled Therapeutic Angiogenesis by Cell Transplantation (TACT) study. They reported that angiogenic cell therapy using BM-MNCs could induce long-term improvement in limb ischemia, leading to extension of amputation-free interval. Implantation of BM-MNCs, including CD34$^+$ EPCs, into ischemic limbs has been examined to increase collateral vessel formation in preclinical and clinical studies. Takeishi-Yuyama reported efficacy and safety of autologous implantation of BM-MNCs in patients with ischemic limb due to PAD.[5] Their primary outcomes were safety and feasibility of treatment, based on ankle-brachial index (ABI) and rest pain, and analysis was per protocol. ABI was calculated by measuring two blood pressures (P*leg*: the systolic blood pressure of dorsalis pedis

---

* To whom correspondence should be addressed.   e-mail: yamaguch@nihs.go.jp

or posterior tibial arteries; and P*arm*. the highest of the left and right arm brachial systolic blood pressure); ABI*leg*=P*leg*/ P*arm*. They suggested that autologous implantation of BM-MNCs could be safe and effective for achievement of therapeutic angiogenesis, because of the natural ability of bone marrow cells to supply EPCs and to secrete various angiogenic factors or cytokines.

Collection of BM-MNCs incurs a risk and is invasive for patients. Several attempts to collect CD34⁺ cells from peripheral blood of patients have been conducted. Since G-CSF is well known to mobilize HSCs from bone marrow to peripheral blood, peripheral blood MNC fraction containing G-CSF-mobilized CD34⁺ cells has been used for the treatment of ischemic disease.[6-8] Huang et al. reported a randomized trial designed to compare patients implanted with G-CSF-mobilized MNCs (group A) *versus* BM-MNC (group B) over a follow-up period of 12 weeks. Comparative analysis revealed that at 12 weeks after cell implantation, improvement of ABI, skin temperature, and rest pain was significantly better in group A patients than group B patients. There was no significant difference between the groups for pain-free walking distance, transcutaneous oxygen pressure, ulcers, and rate of lower limb amputation. They concluded that autologous transplantation of either G-CSF-mobilized peripheral blood (PB)-MNC or BM-MNC significantly promotes improvement of limb ischemia.

Horie et al.[8] described the clinical effects of G-CSF-mobilized autologous PB-MNC in patients with critical limb ischemia. To investigate the long-term clinical outcomes of PB-MNC implantation, they reviewed data for 162 consecutive patients with limb ischemia who received this treatment at 6 hospitals. Significant negative prognostic factors associated with overall survival were concurrent ischemic heart disease and collection of a small number of CD34⁺ cells.

2.2. Mononuclear Cells and Myocardial Infarction
Myocardial infarction is a typical ischemic disease. Dimmeler et al.[9] reported that in patients with acute myocardial infarction, clinical studies preferentially used adult bone marrow-derived cells. Most of the studies suggested that cell therapy reduced infarct size and improved cardiac contractile function.

Flow cytometry analysis revealed[10] that circulating lineage-committed EPCs and CD34⁺ cell counts significantly increased in patients with acute myocardial infarction (*n*=16), peaking on day 7 after onset, whereas they were unchanged in control subjects (*n*=8) who had no evidence of cardiac ischemia, suggesting that lineage-committed EPCs and CD34⁺ cells, their putative precursors, are mobilized during an acute ischemic event in humans. Kocher et al.[11] showed that bone marrow from adult humans contains endothelial precursors with phenotypic and functional characteristics of embryonic hemangioblasts, and that these can be used directly to induce new blood vessel formation in the infarct-bed (vasculogenesis) and proliferation of preexisting vasculature (angiogenesis) after experimental myocardial infarction. The use of G-CSF-mobilized autologous human bone-marrow-derived angioblasts for revascularization of infarcted myocardium has the potential significantly to reduce morbidity and mortality associated with left ventricular remodeling.

3. CELL THERAPY FOR ISCHEMIC DISEASES WITH SELECTED CELLS

Schatteman et al.[12] using diabetic mouse as vascularization model reported that CD34⁺ cells derived from type 1 diabetic humans produced fewer differentiated endothelial cells in culture than did their type 2 diabetic- or non-diabetic-derived counterparts. Li et al.[13] compared the effects of G-CSF-mobilized PB-MNCs and CD34⁺ cell-depleted G-CSF-mobilized PB-MNCs in an ischemia model of athymic nude mice. The capillary density was markedly increased and the rate of limb loss significantly reduced in cell-transplanted groups compared with control. In comparison with G-CSF-mobilized PB-MNCs, the therapeutic efficacy of G-CSF-mobilized PB-MNCs deprived of CD34⁺ cells was impaired, suggesting usefulness of CD34⁺ cells in neovascularization. Therefore selected CD34⁺ cells may be expected to contribute to vascularization in the treatment of other ischemic diseases such as peripheral ischemia (limb) or cerebral ischemia.

While the active cells in bone marrow-derived and G-CSF-mobilized MNCs for the treatment of limb ischemia or myocardial infarction are believed CD34⁺ cells or CD34⁺/KDR⁺ EPCs, these MNCs contain heterogeneous blood cells. Yoon et al.[14] conducted an experiment in rats receiving intra-myocardial injection of either 7×10^5 DiI-labeled total BM cells (TBMCs), the same number of DiI-labeled, clonally expanded BM multipotent stem cells, or the same volume of phosphate-buffered saline in the peri-infarct area. Histological examination with hematoxylin and eosin staining and von Kossa staining confirmed the presence of extensive intra-myocardial calcification, suggesting that direct transplantation of unselected BM cells into the acutely infarcted myocardium may induce significant intra-myocardial calcification in TBMCs rat. Rosenzweig[15] struck a note of warning against using intra-coronary BM-MNCs in acute myocardial infarction.

Kawamoto et al.[16] suggested that in myocardial infarction CD34⁺ cells exhibit superior efficacy for preserving myocardial integrity and function than unselected circulating MNCs. Similarly, two clinical trials comparing unselected MNCs with selected CD34⁺/CXCR4⁺ cells (EPCs) in patients with acute myocardial infarction (AMI)[17,18] were conducted. In patients with AMI who despite timely and successful treatment with primary PCI developed impairment of the left ventricular ejection fraction (LVEF), treatment with either selected or non-selected BMCs did not lead to significant improvement of LVEF. There was, however, a trend in favor of cell therapy, particularly in patients with most severely impaired LVEF and longer delay between the symptoms and revascularization, which is considered the high-risk group. Use of selected CD34⁺/CXCR4⁺ cells in patients with significantly reduced LV function is safe, feasible, and warrants further investigation.

On the other hand, a recent *meta*-analysis of 18 randomized controlled trials attempted to define the long-term impact of progenitor cell therapy in the treatment of myocardial infarction.[19] A total of 980 patients from 18 studies were analyzed. Following BM-MNC transplantation, regional myocardial anatomy displayed statistically and clinically significant improvements compared with controls, albeit without functional changes. BM-MNC transplantation for myocardial infarction was able to deliver benefits over regular therapy even at 18-month follow-up, particularly when used to treat AMI. CD34⁺

cell therapy holds promise for myocardial infarction treatment in the future. The study did not clarify any superiority difference between BM-MNCs and selected CD34$^+$ cells for the treatment of myocardial infarction.

Generally, CD34$^+$ cells that are purified from BM-MNCs or PB-MNCs contain HSC and EPC. During culture, CD34$^+$ cells form multiple cell clusters and EPC-like attaching cells with endothelial cell lineage markers (CD31, vascular endothelial cadherin).[10] The major population of collected CD34$^+$ cells does not express CD31 and other endothelial cell markers, suggesting that they can differentiate into EPCs. Therefore administered CD34$^+$ cells may be expected to differentiate into EPCs, which could contribute to vascularization. A challenge to develop CD34$^+$ cell therapy for ischemic diseases is a relative low basal density of CD34$^+$ cells in the circulation. Although G-CSF is well known to mobilize CD34$^+$ cells from bone marrow into circulation, the concentration of mobilized CD34$^+$ cells may not be enough to treat ischemia.

4. IN VITRO INDUCTION AND EXPANSION OF EPCs

Whereas cell therapy using EPCs has been widely performed to rescue tissue damage due to critical ischemia, the population of EPCs that can be purified from PB-MNCs or BM-MNCs is limited. Therefore in vitro expansion and differentiation of EPCs have been attempted.[20]

EPCs are thought derived from several kinds of cells; cells characterized as CD34$^+$/AC133$^+$/CD14$^+$ are also thought to differentiate into EPCs. EPCs may release angiogenic factors such as interleukin-8 (IL-8), G-CSF, hepatocyte growth factor, and vascular endothelial growth factor (VEGF). To obtain a sufficient number of EPCs for treatment purposes may be very important in cell therapy for critical ischemia.

4.1. Endothelial Progenitor Cells Derived from CD34$^+$ or AC133$^+$ Cells EPCs were first isolated as CD34$^+$ cells, and magnetically sorted CD34$^+$ cells containing HSCs differentiated into endothelial cells in vitro.[1] CD34$^+$ cells are thought to stimulate angiogenesis either by their ability to differentiate into endothelial cells or by enhancing the formation and repair of endothelium and vascularization through paracrine stimuli.[1,21-25] AC133-positive cells, which are typical HSCs, also can differentiate into EPCs and endothelial cells. A challenge for development for cell therapy using EPCs or endothelial cells is to collect sufficient amounts of EPCs or cell sources for EPC/endothelial cells. EPCs are thought derived from CD34$^+$ or AC133$^+$ cells that do not express endothelial-lineage markers. If CD34$^+$ cells collected from peripheral blood or BM-MNCs are expanded and efficiently differentiated into EPCs in vitro, sufficient amounts of EPC could be obtained for the treatment of ischemic diseases.

A common barrier against characterization and subsequent utilization of putative EPCs is the poor number of cells obtained after purification from peripheral or cord blood. EPCs represent a very small subset of PB-MNCs, ranging at 0.002–0.01% in peripheral blood and 0.2–1% in umbilical cord blood.[12] According to the cell numbers that have been used for systemic infusion of allogenic EPCs in patients,[17,18] this would have required a significant amount of blood if the cells were not previously expanded in vitro.[5]

Factors affecting expansion and differentiation of EPCs are thought to include several endothelial cell growth factors

such as VEGF and fibroblast growth factor (FGF) and cytokines such as c-kit, Flt-3, IL-3, and IL-6. Other cytokines are thought to contribute to expansion of HSCs, suggesting that expanded HSCs will differentiate into EPCs. Growth factors are essential for proliferation, differentiation and function of endothelial cells. These biological cocktails may stimulate the propagation of HSCs of which partial populations can differentiate into EPCs.

The extracellular matrix (ECM) may also affect in vitro expansion and differentiation of EPCs from CD34$^+$ or AC133$^+$ cells. ECM is critical for all aspects of vascular biology. Vascular endothelial cells require adhesion to ECM for migration; endothelial cells migration is important for angiogenesis, particularly during sprouting of new blood vessels from existing vasculature. Evidence from in vitro experiments indicates that many of the interstitial and provisional ECM components that are encountered during angiogenesis including interstitial fibrin and collagen I are capable of supporting chemotactic migration.

On the other hand, in vitro induction and expansion of EPCs to form HSCs (CD34$^+$ or AC133$^+$ cells) have been reported efficiently induced on fibronectin (FN) as ECM. As judged by positive staining for endothelial markers vWF and VE-cadherin, the combination of VEGF with FN produced significantly more endothelial colonies than collagens I or IV or vitronectin.[26,27] Considering that FN also enhanced VEGF-mediated CD34$^+$ cell migration, Wijelath et al. concluded that VEGF and FN together significantly promote migration and differentiation of CD34$^+$ cells into EPCs. These results also indicate that essential ECM for the induction and expansion EPCs is different from mature endothelial cells.

Concerning induction of EPCs, thrombopoietin (TPO) is reported to enhance proliferation of EPCs from AC133$^+$ cells. TPO is a well-known cytokine for megakaryocyte growth and development factor. Collected AC133$^+$ HSC cells do not express TPO receptor. When AC133$^+$ cells were cultivated in the condition of EPC differentiation, a part of AC133$^+$ cells expressed TPO receptor and markedly proliferated (Fig. 1). TPO induced a fourfold increase in EPCs (CD31^{bright} cells). This result suggests that efficient induction of EPCs in vitro with TPO contributes further to development of cell therapy for critical ischemic diseases.

4.2. Early and Late EPCs At first, EPCs were thought a source of endothelial cells.[1] A number of studies have described therapeutic applications of EPCs against ischemic diseases. Two types of EPCs have been described in vitro; early EPCs and late EPCs (also called endothelial outgrowth

Table 1. Comparison of Early EPC and Late EPC (Out Growth EPC: OEC)

	Early EPC	OEC
Morphology	Spindle shape	Cobble stone
Appearance	1w–3w	3w–
Proliferation	Low	High
Vessel formation in matrigel	Negative or weak	Positive
Cytokine release	High	Low
Cell (surface) marker	CD31, eNOS KDR, CD14, VE cadherin (weak)	CD31, eNOS KDR, VE cadherin

A
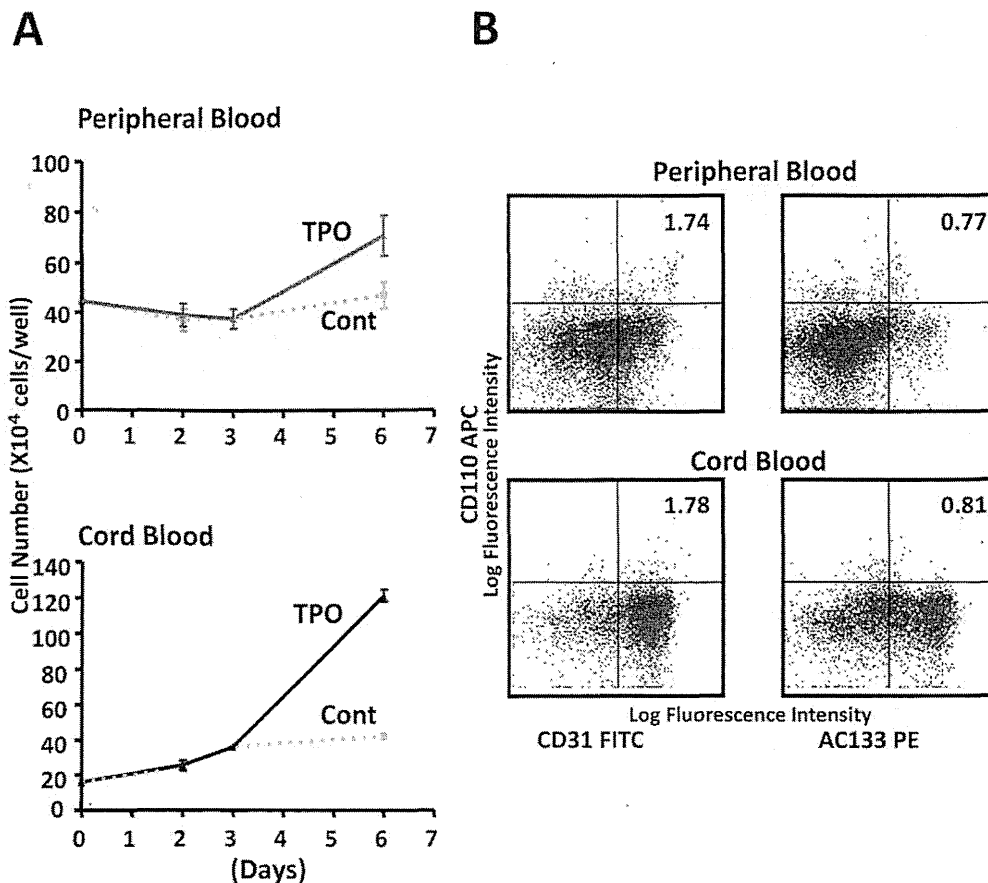
B

Peripheral Blood

Fig. 1. Time–Course Analysis of TPO-Treated AC133⁺ Cells and Expression of TPO Receptor (CD110)

Alteration of cell number was counted at 2, 3, and 6 d. Solid and dotted lines indicate TPO-treated cells and control (VEGF alone) cells, respectively. The results represent mean±S.E. of triplicate wells. (B) Flow cytometric analysis of CD110 expression on AC133⁻ cells cultured for 3 d. The y-axis represents log fluorescence intensity of CD110-APC; x-axis, CD31-FITC (left panels) and AC133-PE (right panels). The number in the flow cytometric dot blot indicates the percent CD110⁻CD31⁻ and CD110⁻AC133⁺ populations, respectively. Upper panels, peripheral blood; lower panels, cord blood (*J. Biol. Chem.*, Kanayasu-Toyoda *et al.*, 2007).
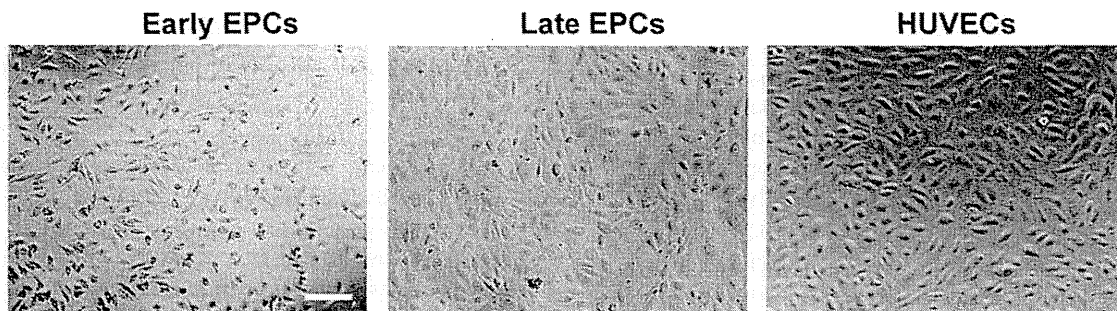
Fig. 2. Comparison of Morphology of Early EPCs, Late EPCs, and HUVECs

Morphology of early EPCs (left), late EPCs (middle), and HUVECs (right) by microscopy. Scale bar, 100 μm.

cells) (Table 1). Although early EPCs and late EPCs express common features such as expression of CD31, LDL uptake, and other endothelial markers, they have distinct characteristics with respect to morphology (Fig. 2), proliferation ability, and *in vitro* function such as vascular tube formation.[25,28–31] The characteristics of early EPCs are different from typical endothelial phenotype; for example they exhibit weak ability for neovascularization *in vitro*, but early EPCs produce angiogenic paracrine factors.[32]

During *in vitro* culture of CD34⁺ or AC133⁺ cells, early EPCs appeared relatively rapidly (within 1 weak) as fibroblastic cells that express CD31, KDR, or other endothelial lineage

marker. The appearance of late EPCs is delayed in comparison with that of early EPCs, and these cells' proliferation ability is much higher than that of either endothelial cells or early EPCs. The different abilities of these EPCs suggest the hypothesis that early EPCs migrate into ischemic regions and contribute to vascularization by recruiting circulating endothelial cells whereas late EPCs secrete angiogenic factors and thus integrate into neovascularizaion. This synergistic model remains to be fully elucidated.

The origin of EPCs raises controversial discussion.[33] Concerning the origin of early EPCs, Rehman *et al.*[25] reported that these cells are derived from monocytes/macrophages

and secrete angiogenic growth factors. The reasoning of this hypothesis is that early EPCs express not only endothelial lineage markers but also CD45, common leukocyte antigen. Timmermans et al. reported that the CD34^{+}/CD45^{+} HSC cell fraction did not generate late EPCs, but differentiated into EC-like cells through a CD14^{+} monocytic pathway.[34] On the other hand, Kanayasu-Toyoda et al. reported that early EPCs are differentiated from AC133^{+} cells not through CD14 expression. The precise origin of early EPCs needs further investigation.

5. CONCLUSION

Cell therapies for severe ischemic diseases have been developed alongside clarification of the biology of EPCs. Many sources of EPCs have been proposed; MNCs fraction containing CD34^{+} or CD133^{+}, isolated CD34^{+} and AC133^{+} cell, and in vitro induction and differentiation EPCs from HSCs. Many in vitro, in vivo, and clinical studies have looked at these cells. However, the origin of these cells remains to be elucidated, and in vivo mechanisms by which EPCs contribute to neovascularization should be clarified in future.

REFERENCES

1) Asahara T, Murohara T, Sullivan A, Silver M, van der Zee R, Li T, Witzenbichler B, Schatteman G, Isner JM. Isolation of putative progenitor endothelial cells for angiogenesis. Science, 275, 964–967 (1997).

2) Shi Q, Rafii S, Wu MH, Wijelath ES, Yu C, Ishida A, Fujita Y, Kothari S, Mohle R, Sauvage LR, Moore MA, Storb RF, Hammond WP. Evidence for circulating bone marrow-derived endothelial cells. Blood, 92, 362–367 (1998).

3) Fadini GP, Losordo D, Dimmeler S. Critical reevaluation of endothelial progenitor cell phenotypes for therapeutic and diagnostic use. Circ. Res., 110, 624–637 (2012).

4) Matoba S, Tatsumi T, Murohara T, Imaizumi T, Katsuda Y, Ito M, Saito Y, Uemura S, Suzuki H, Fukumoto S, Yamamoto Y, Onodera R, Teramukai S, Fukushima M, Matsubara H, TACT Follow-up Study Investigators. Long-term clinical outcome after intramuscular implantation of bone marrow mononuclear cells (Therapeutic Angiogenesis by Cell Transplantation [TACT] trial) in patients with chronic limb ischemia. Am. Heart J., 156, 1010–1018 (2008).

5) Tateishi-Yuyama E, Matsubara H, Murohara T, Ikeda U, Shintani S, Masaki H, Amano K, Kishimoto Y, Yoshimoto K, Akashi H, Shimada K, Iwasaka T, Imaizumi T, Therapeutic Angiogenesis using Cell Transplantation (TACT) Study Investigators. Therapeutic angiogenesis for patients with limb ischaemia by autologous transplantation of bone-marrow cells: a pilot study and a randomised controlled trial. Lancet, 360, 427–435 (2002).

6) Onodera R, Teramukai S, Tanaka S, Kojima S, Horie T, Matoba S, Murohara T, Matsubara H, Fukushima M, BMMNC Follow-Up Study Investigators M-PBMNC Follow-Up Study Investigators. Bone marrow mononuclear cells versus G-CSF-mobilized peripheral blood mononuclear cells for treatment of lower limb ASO: pooled analysis for long-term prognosis. Bone Marrow Transplant., 46, 278–284 (2011).

7) Huang PP, Yang XF, Li SZ, Wen JC, Zhang Y, Han ZC. Randomised comparison of G-CSF-mobilized peripheral blood mononuclear cells versus bone marrow-mononuclear cells for the treatment of patients with lower limb arteriosclerosis obliterans. Thromb. Haemost., 98, 1335–1342 (2007).

8) Horie T, Onodera R, Akamastu M, Ichikawa Y, Hoshino J, Kaneko E, Iwashita C, Ishida A, Tsukamoto T, Teramukai S, Fukushima M, Kawamura A, Japan Study Group of Peripheral Vascular Regeneration Cell Therapy (JPRCT). Long-term clinical outcomes for patients with lower limb ischemia implanted with G-CSF-mobilized autologous peripheral blood mononuclear cells. Atherosclerosis, 208, 461–466 (2010).

9) Dimmeler S, Burchfield J, Zeiher AM. Cell-based therapy of myocardial infarction. Arterioscler. Thromb. Vasc. Biol., 28, 208–216 (2008).

10) Shintani S, Murohara T, Ikeda H, Ueno T, Honma T, Katoh A, Sasaki K, Shimada T, Oike Y, Imaizumi T. Mobilization of endothelial progenitor cells in patients with acute myocardial infarction. Circulation, 103, 2776–2779 (2001).

11) Kocher AA, Schuster MD, Szabolcs MJ, Takuma S, Burkhoff D, Wang J, Homma S, Edwards NM, Itescu S. Neovascularization of ischemic myocardium by human bone-marrow-derived angioblasts prevents cardiomyocyte apoptosis, reduces remodeling and improves cardiac function. Nat. Med., 7, 430–436 (2001).

12) Schatteman GC, Hanlon HD, Jiao C, Dodds SG, Christy BA. Blood-derived angioblasts accelerate blood-flow restoration in diabetic mice. J. Clin. Invest., 106, 571–578 (2000).

13) Li S, Zhou B, Han ZC. Therapeutic neovascularization by transplantation of mobilized peripheral blood mononuclear cells for limb ischemia. A comparison between CD34^{+} and CD34-mononuclear cells. Thromb. Haemost., 95, 301–311 (2006).

14) Yoon YS, Park JS, Tkebuchava T, Luedeman C, Losordo DW. Unexpected severe calcification after transplantation of bone marrow cells in acute myocardial infarction. Circulation, 109, 3154–3157 (2004).

15) Rosenzweig A. Cardiac cell therapy—mixed results from mixed cells. N. Engl. J. Med., 355, 1274–1277 (2006).

16) Kawamoto A, Iwasaki H, Kusano K, Murayama T, Oyamada A, Silver M, Hulbert C, Gavin M, Hanley A, Ma H, Kearney M, Zak V, Asahara T, Losordo DW. CD34-positive cells exhibit increased potency and safety for therapeutic neovascularization after myocardial infarction compared with total mononuclear cells. Circulation, 114, 2163–2169 (2006).

17) Tendera M, Wojakowski W, Ruzyllo W, Chojnowska L, Kepka C, Tracz W, Musialek P, Piwowarska W, Nessler J, Buszman P, Grajek S, Breborowicz P, Majka M, Ratajczak MZ, REGENT Investigators. Intracoronary infusion of bone marrow-derived selected CD34^{+}CXCR4^{+} cells and non-selected mononuclear cells in patients with acute STEMI and reduced left ventricular ejection fraction: results of randomized, multicentre Myocardial Regeneration by Intracoronary Infusion of Selected Population of Stem Cells in Acute Myocardial Infarction (REGENT) Trial. Eur. Heart J., 30, 1313–1321 (2009).

18) Mackie AR, Losordo DW. CD34-positive stem cells: in the treatment of heart and vascular disease in human beings. Tex. Heart Inst. J., 38, 474–485 (2011).

19) Jiang M, He B, Zhang Q, Ge H, Zang MH, Han ZH, Liu JP, Li JH, Zhang Q, Li HB, Jin Y, He Q, Gong XR, Yin XY. Randomized controlled trials on the therapeutic effects of adult progenitor cells for myocardial infarction: meta-analysis. Expert Opin. Biol. Ther., 10, 667–680 (2010).

20) Ahrens I, Domeij H, Topcic D, Haviv I, Merivirta RM, Agrotis A, Leitner E, Jowett JB, Bode C, Lappas M, Peter K. Successful in vitro expansion and differentiation of cord blood derived CD34^{+} cells into early endothelial progenitor cells reveals highly differential gene expression. PLoS ONE, 6, e23210 (2011).

21) Dimmeler S. Regulation of bone marrow-derived vascular progenitor cell mobilization and maintenance. Arterioscler. Thromb. Vasc. Biol., 30, 1088–1093 (2010).

22) Hirschi KK, Ingram DA, Yoder MC. Assessing identity, phenotype, and fate of endothelial progenitor cells. Arterioscler. Thromb. Vasc. Biol., 28, 1584–1595 (2008).

23) Hristov M, Erl W, Weber PC. Endothelial progenitor cells: mobilization, differentiation, and homing. Arterioscler. Thromb. Vasc.

Biol., **23**, 1185–1189 (2003).

24) Jujo K, Ii M, Losordo DW. Endothelial progenitor cells in neovascularization of infarcted myocardium. *J. Mol. Cell. Cardiol.*, **45**, 530–544 (2008).

25) Rehman J, Li J, Orschell CM, March KL. Peripheral blood "endothelial progenitor cells" are derived from monocyte/macrophages and secrete angiogenic growth factors. *Circulation*, **107**, 1164–1169 (2003).

26) Wijelath ES, Rahman S, Murray J, Patel Y, Savidge G, Sobel M. Fibronectin promotes VEGF-induced CD34 cell differentiation into endothelial cells. *J. Vasc. Surg.*, **39**, 655–660 (2004).

27) Kanayasu-Toyoda T, Yamaguchi T, Oshizawa T, Hayakawa T. CD31 (PECAM-1)-bright cells derived from AC133-positive cells in human peripheral blood as endothelial-precursor cells. *J. Cell. Physiol.*, **195**, 119–129 (2003).

28) Bompais H, Chagraoui J, Canron X, Crisan M, Liu XH, Anjo A, Tolla-Le Port C, Leboeuf M, Charbord P, Bikfalvi A, Uzan G. Human endothelial cells derived from circulating progenitors display specific functional properties compared with mature vessel wall endothelial cells. *Blood*, **103**, 2577–2584 (2004).

29) Lin Y, Weisdorf DJ, Solovey A, Hebbel RP. Origins of circulating endothelial cells and endothelial outgrowth from blood. *J. Clin. Invest.*, **105**, 71–77 (2000).

30) Yoder MC, Mead LE, Prater D, Krier TR, Mroueh KN, Li F, Krasich R, Temm CJ, Prchal JT, Ingram DA. Redefining endothelial progenitor cells *via* clonal analysis and hematopoietic stem/progenitor cell principals. *Blood*, **109**, 1801–1809 (2007).

31) Yoon CH, Hur J, Park KW, Kim JH, Lee CS, Oh IY, Kim TY, Cho HJ, Kang HJ, Chae IH, Yang HK, Oh BH, Park YB, Kim HS. Synergistic neovascularization by mixed transplantation of early endothelial progenitor cells and late outgrowth endothelial cells: the role of angiogenic cytokines and matrix metalloproteinases. *Circulation*, **112**, 1618–1627 (2005).

32) Kanayasu-Toyoda T, Ishii-Watabe A, Suzuki T, Oshizawa T, Yamaguchi T. A new role of thrombopoietin enhancing *ex vivo* expansion of endothelial precursor cells derived from AC133-positive cells. *J. Biol. Chem.*, **282**, 33507–33514 (2007).

33) Urbich C, Dimmeler S. Endothelial progenitor cells: characterization and role in vascular biology. *Circ. Res.*, **95**, 343–353 (2004).

34) Timmermans F, Van Hauwermeiren F, De Smedt M, Raedt R, Plasschaert F, De Buyzere ML, Gillebert TC, Plum J, Vandekerckhove B. Endothelial outgrowth cells are not derived from CD133⁺ cells or CD45⁺ hematopoietic precursors. *Arterioscler. Thromb. Vasc. Biol.*, **27**, 1572–1579 (2007).

Yuji Inoue, Ritsuko Kubota-Koketsu, Akifumi
Yamashita, Mitsuhiro Nishimura, Shoji Ideno,
Ken-ichiro Ono, Yoshinobu Okuno and
Kazuyoshi Ikuta

Access the most updated version of this article at doi: 10.1074/jbc.M112.420547

Find articles, minireviews, Reflections and Classics on similar topics on the JBC Affinity Sites.

Alerts:
• When this article is cited
• When a correction for this article is posted

Click here to choose from all of JBC's e-mail alerts

Supplemental material:
http://www.jbc.org/content/suppl/2012/12/21/M112.420547.DC1.html

This article cites 23 references, 5 of which can be accessed free at
http://www.jbc.org/content/288/7/4981.full.html#ref-list-1

Induction of Anti-influenza Immunity by Modified Green Fluorescent Protein (GFP) Carrying Hemagglutinin-derived Epitope Structure*[S]

Yuji Inoue[‡1], Ritsuko Kubota-Koketsu[‡§], Akifumi Yamashita[¶], Mitsuhiro Nishimura[‡], Shoji Ideno[||], Ken-ichiro Ono[**], Yoshinobu Okuno[§], and Kazuyoshi Ikuta[‡]

From the [‡]Department of Virology, Research Center for Infectious Diseases Control, Research Institute of Microbial Diseases, and the [¶]Department of Genome Informatics, Genome Information Research Center, Research Institute of Microbial Diseases, Osaka University, Suita, Osaka 565-0871, Japan, the [§]Kanonji Institute, Research Foundation for Microbial Diseases of Osaka University, Kanonji, Kagawa, 768-0061, Japan, the [||]Infectious Pathogen Research Group, Osaka Laboratory, Benesis Corporation, Osaka 532-8505, Japan, and the [**]Ina Laboratory, Medical and Biological Laboratories Corporation, Ltd., Ina, Nagano, 396-0002, Japan

Background: Rapidly producible vaccines are desired for forthcoming influenza pandemics.

Results: Anti-influenza immunity was induced by modified GFP exposing residues from a conserved β-sheet-type hemagglutinin epitope.

Conclusion: A novel strategy for immunization targeting conformational epitopes was established by mimicking the epitope structure.

Significance: Because of its instant producibility, this type of immunogen meets the requirement for next-generation influenza vaccines.

The development of vaccination methods that can overcome the emergence of new types of influenza strains caused by escape mutations is desirable to avoid future pandemics. Here, a novel type of immunogen was designed that targeted the conformation of a highly conserved region of influenza A virus hemagglutinin (HA) composed of two separate sequences that associate to form an anti-parallel β-sheet structure. Our previous study identified this β-sheet region as the structural core in the epitope of a characteristic antibody (B-1) that strongly neutralizes a wide variety of strains within the H3N2 serotype, and therefore this β-sheet region was considered a good target to induce broadly reactive immunity against the influenza A virus. To design the immunogen, residues derived from the B-1 epitope were introduced directly onto a part of enhanced green fluorescent protein (EGFP), whose surface is mostly composed of β-sheets. Through site-directed mutagenesis, several modified EGFPs with an epitope-mimicking structure embedded in their surface were prepared. Two EGFP variants, differing from wild-type (parental) EGFP by only five and nine residues, induced mice to produce antibodies that specifically bind to H3-type HA and neutralize H3N2 virus. Moreover, three of five mice immunized with each of these EGFP variants followed by a booster with equivalent mCherry variants acquired anti-viral immunity against challenge with H3N2 virus at a lethal dosage. In contrast to conventional methods, such as split HA vaccine, preparation of this type of immunogen requires less time and is

therefore expected to be quickly responsive to newly emerged influenza viral strains.

Humankind has encountered a number of influenza pandemics. In addition, frequently emerging minor mutations of a vaccine target may also interrupt our efforts to prevent influenza. Generally, influenza vaccine manufacturing takes months (1), approximately half a year for egg-grown virus and at least 2 months for cell culture-grown virus. Such latencies may cause severe problems, especially in pandemics. For example, in the case of the most recent swine-origin pandemic influenza A in 2009 (H1N1pdm) (2), serious concerns arose in countries in the southern hemisphere, such as Australia, because the outbreak occurred immediately before the influenza season (3). To overcome such limitations of conventional vaccination methods, there is a need to develop new methods that can be instantly updateable to newly emerged viral strains and/or induce viral neutralization antibodies that target highly conserved regions.

In a previous study, we succeeded in isolating several clones of human-type monoclonal antibodies produced by hybridoma established from peripheral blood mononuclear cells of influenza-vaccinated volunteers (4). Among them, one notable antibody clone, named B-1, demonstrated high neutralization titers against a wide variety of influenza A viral strains belonging to the H3N2 serotype, including strains isolated more than 40 years ago. Through an epitope-mapping study using synthetic oligopeptides, B-1 antibody was shown to recognize a region of hemagglutinin (HA) protein composed of two separate sequences spanning residues 167–187 and 225–241 (supplemental Fig. S1). According to the known crystal structure of HA, these two subregions appear to associate with each other through an anti-parallel β-sheet structure to form one epitope region located beneath the receptor-binding site (supplemental

Fig. S1). Phylogenic analysis indicated that these sequences and their corresponding sequences in other HA serotypes, including H1N1pdm, are highly conserved in a serotype-dependent manner, suggesting that their broad neutralizing properties have arisen from this high conservation (5). Particularly, the β-sheet portion composed of two sequences spanning residues 175–184 and 229–238 (called the "upper" and "lower" subregions, respectively) appears to be highly conserved; DKLYI-WGVHH occupies 97.8% of the upper subregion, and RISI-YWTIVK occupies 94.5% of the lower subregion among 12,879 HA sequences of H3N2 strains isolated from human within the past 43 years.

A similar broadly neutralizing antibody clone, named D-1, has also been established from another donor's peripheral blood mononuclear cells and, interestingly, recognizes a region almost identical to that of B-1 (4). Currently, vaccinations with synthetic oligopeptide(s) corresponding to highly conserved epitopes are widely applied to produce antibodies that protect against a broad range of viral strains (6, 7). Because B-1 and D-1 were the strongest and the broadest neutralizing antibodies among those isolated from the peripheral blood mononuclear cell population of each vaccinee, the B-1 (D-1) epitope, which has not to our knowledge been previously mapped, was thought to be an attractive candidate target for peptide-based vaccines. Thus, we tested the ability of synthetic oligopeptides corresponding to the epitope sequences to induce the production of neutralizing antibodies against influenza virus. When peripheral blood mononuclear cells from human vaccinees were stimulated by the oligopeptide(s) *ex vivo*, we observed production of antibodies with viral neutralizing activity,[2] indicating that oligopeptide stimulation may be effective for individuals that already have certain memories. However, our attempt to immunize naive animals with the synthetic oligopeptide(s) to induce production of virus-neutralizing antibodies appeared less successful,[3] probably because the antigenicity for primary immunity was highly dependent on the conformation of the epitope. In addition, according to previously determined crystal structure models, this epitope region appears mostly buried within the stable HA trimer (supplemental Fig. S1), and therefore immunization with intact HA would not be so effective to target this region, although B-1 and D-1 were probably raised against HA in vaccines.

In this study, to induce antibodies specifically recognizing this region, we designed immunogens using a novel strategy focusing on secondary structure. The basic strategy was to build an epitope-mimicking structure directly on the surface of an epitope carrier protein that originally exposes anti-parallel β-sheet structure. The model carrier proteins we selected here are two fluorescent proteins: enhanced green fluorescent protein (EGFP)[4] and mCherry (8). Despite the rather low overall similarity between their sequences, their overall structures are

quite similar, with 11 β-strands on the surface surrounding the fluorophore to form a barrel-like structure. Utilizing this scaffold, the epitope-derived residues were introduced directly onto the surface of EGFP and mCherry by site-directed mutagenesis. We prepared four variants for each carrier protein. By using these as immunogens, we tested the induction of anti-HA antibody production and the acquisition of anti-influenza immunity. Using monoclonal antibodies isolated from mice immunized with the modified EGFPs, we also evaluated their viral neutralization activities.

EXPERIMENTAL PROCEDURES

Reagents—As a positive control for immunization, a seasonal influenza vaccine, Biken HA (Research Foundation for Microbial Diseases of Osaka University, Kanonji, Japan), containing a mixture of HA-enriched extracts from A/Brisbane/59/2007 (H1N1), A/Uruguay/716/2007 (H3N2), and B/Brisbane/60/2008 strains, was used at 100 μl/body. As an ELISA antigen to test anti-HA reactivity, HA-enriched split vaccine prepared from A/Hiroshima/52/2005 (H3N2) virus was used. As a probe for cell infection by influenza A virus, anti-influenza-A NP antibody C43 (Abcam) was used (9).

Design of Variant EGFPs—The β-strands of EGFP to which HA-derived residues were introduced were determined mainly through the evaluation of the structural similarity between α-carbons (Cα) from HA and EGFP in their crystal structure (Protein Data Bank accession numbers 2VIU and 1EMA, respectively), which was estimated by the root mean square value calculated using PyMOL software (DeLano Scientific).

Mutagenesis—The oligonucleotides used for mutagenesis are summarized in supplemental Table S1. All PCRs were performed with KOD Plus DNA polymerase (Toyobo). The ORFs of pEGFP-N and pmCherry-N (Clontech) were previously subcloned onto pET-28a(+) plasmid vector (Merck Millipore) to produce pET-EGFP and pET-mCherry, respectively. Using each plasmid as a template, fragments containing the sequences corresponding to N-terminal and C-terminal halves of EGFP or mCherry were amplified by PCR with primer pairs P1/P2 and P3/P4, respectively. In the course of this PCR step, mutations were introduced by primers P2 and P3. These two fragments were combined by PCR with the P1/P4 primer pair. The combined fragment was subcloned onto the pET28a vector (Novagen) using NdeI and EcoRI restriction sites. UL1 variants were produced by introducing L1 mutations into the U1 variants.

Protein Expression—*Escherichia coli* Rosetta (DE3) pLysS (EMD Millipore) cells were transformed by each plasmid prepared as described above. Transformed cells were cultured in LB (plus kanamycin) medium at 37 °C. When the optical density at 600 nm reached 0.5, protein expression was induced by the addition of 0.2 mM isopropyl-1-thio-β-D-galactopyranoside. Importantly, the culturing temperature should be changed to 18 °C immediately after the isopropyl-1-thio-β-D-galactopyranoside addition because the maturation of several variants of EGFP or mCherry was found to be inefficient with standard culture at 37 °C. Cell culture was continued overnight. If EGFP or mCherry and their variants were expressed successfully, the collected cell pellet would already appear green or purple-red in color, respectively.

---

[2] R. Kubota-Koketsu and K. Ikuta, unpublished data.
[3] S. Ideno, K. Sakai, M. Yunoki, R. Kubota-Koketsu, Y. Inoue, S. Nakamura, T. Yasunaga, and K. Ikuta, submitted for publication.
[4] The abbreviations used are: EGFP, enhanced green fluorescent protein; FCA, Freund's complete adjuvant; FRNT, focus reduction neutralization test; proK, proteinase K; RDE, receptor-destroying enzyme; MEM, minimum essential medium.

Protein Purification—After the protein expression, collected *E. coli* cells suspended in PBS containing 0.1 mg/ml lysozyme (Seikagaku Corp.) and 1 mM phenylmethylsulfonyl fluoride (Sigma) were incubated for 30 min on ice and lysed by sonication. After removal of the insoluble fraction by centrifugation, the cell extract was applied onto a nickel-Sepharose Fast Flow (GE Healthcare) column equilibrated with PBS containing 5 mM imidazole. After washing the column with PBS containing 40 mM imidazole, bound protein was eluted by PBS containing 300 mM imidazole. Colored fractions were dialyzed against 20 mM Tris-HCl (pH 8.0) and applied onto a Q Sepharose (GE Healthcare) column equilibrated with 20 mM Tris-HCl (pH 8.0). After washing the column, bound protein was eluted by a 0–200 mM NaCl gradient.

The purity of each fraction was checked with Coomassie Brilliant Blue staining after SDS-PAGE. The EGFP- and mCherry-enriched fractions were collected and dialyzed against PBS. If necessary, protein was concentrated by Centriprep 10k (Millipore). In SDS-PAGE, every variant protein was found to retain its fluorescence in the gel but had a unique mobility when boiling was omitted prior to sample injection (Fig. 1C), whereas almost equal mobility was observed when samples were boiled in SDS (Fig. 2C, without proteinase K treatment). Protein concentration was quantified by the Pierce 660-nm protein assay (Thermo Scientific). In SDS-PAGE of mCherry or its variants purified as described above and boiled in SDS, some extra bands appeared below the full-length protein, whereas very little additional banding appeared in the non-boiled condition. This observation indicates that these samples contain some degraded fragments that cannot be fully separated by column under native conditions because they have been integrated to form the mature mCherry structure.

Circular Dichroism (CD)—Purified wild-type (parental) EGFP and its UL1 and UL2 variants were adjusted to 100 μM in 20 mM Tris-HCl (pH 8.0). Far-UV CD spectra were measured in a 0.1-mm path length cell from 260 to 190 nm using a CD spectrometer (model 202, Aviv Biomedical). All measurements were performed at room temperature under a nitrogen flow.

Protease Resistance and Thermostability Tests—To test protease resistance, EGFP and its variants, each at a final concentration of 100 nM, were incubated with the indicated concentration of proteinase K (proK) for the indicated time at 37 °C. After the incubation, fluorescence was measured with excitation and emission wavelengths at 470 and 507 nm, respectively. To test thermostability, each EGFP or its variant at a final concentration of 100 nM was incubated in the absence or presence of 0.1% SDS for 5 min at the indicated temperature. Fluorescence was measured as described above. Denaturation temperature (T_d) was estimated by fitting the plot to a sigmoidal function, $F = F_{max}/(1 + \exp(p(T_d - T)))$, where F is the fluorescence after heat treatment at T (°C), and F_{max} is the fluorescence without heat treatment. T_d indicates the temperature at which the fluorescence $F = 0.5 \times F_{max}$.

Immunization—To prepare immunogens, each purified variant of EGFP or mCherry was adjusted to the appropriate concentration in PBS and mixed with an equal volume of Freund's complete adjuvant (FCA) or Freund's incomplete adjuvant (Wako) into an emulsion. Emulsion can be formed efficiently by plunging back and forth in two 2.5-ml syringes linked with a three-way stopcock. Immunogen prepared as described above containing 7.5 mg/ml EGFP variant with FCA was inoculated intraperitoneally into female 6-week-old BALB/c mice at 200 μl (1.5 mg)/body. After 3 weeks, booster immunization was performed with the same immunogen. Mice immunized with seasonal influenza vaccine at 100 μl/body were used as a positive control group, and mice immunized with PBS/FCA emulsion were used as a negative control group. After 3 weeks, blood was collected from the tail, and serum was used for tests. Hybridomas described below were prepared from mice immunized in that manner. For virus challenge, immunogen containing 750 or 75 μg/ml EGFP variants was prepared as emulsion with FCA and inoculated into female 5-week-old BALB/c mice at 200 μl (150 or 15 μg)/body. After 2 weeks, antigens prepared with the same concentration of equivalent mCherry variants and Freund's incomplete adjuvant were inoculated intraperitoneally at 200 μl/body as a booster. After a further 2 weeks, influenza A/Guizhou/54/1989 × Puerto Rico/8/1934 (H3N2) mouse-adapted reassortant virus was infected intranasally at 6 × 10² focus-forming units/g body weight.

ELISA—Fifty microliters of 2 μg/ml antigen solution were adsorbed on the bottom of F96 Maxisorp Nunc-Immuno Plates (Thermo Scientific) and incubated overnight at 4 °C. After blocking with PBS containing 25% (v/v) Blocking One (Nacalai Tesque), the plate was reacted with serum or purified antibody appropriately diluted in PBS containing 5% (v/v) Blocking One. After five washes with PBS containing 0.02% Tween 20 (PBS-T), the plate was reacted with HRP-conjugated secondary antibody at a 1:5,000 dilution. After five washes with PBS-T, 50 μl of SureBlue TMB 1-component Microwell Peroxidase Substrate (KPL) was added and incubated at room temperature. Color development was stopped by the addition of 50 μl of 1 M H_2SO_4, and optical density at 450 nm was measured.

Hybridoma Preparation—Mice that exhibited sera with a high content of HA-reactive antibodies and high viral neutralization titers were finally boosted by intraperitoneal inoculation with the equivalent variant of mCherry without adjuvant at 0.2 mg/body. After 3 days, splenocytes were collected and fused with mouse myeloma PAI cells by a standard polyethylene glycol fusion method. Fused cells were cultured on 5 × 96-well plates at 100 μl/well. After forming colonies, culture supernatants were tested by ELISA against either HA vaccine prepared from A/Hiroshima/52/2005 (H3N2) virus or EGFP. Cells containing HA-reactive clones were diluted to 10–50 cells/ml and mixed with fresh splenocytes from a naive mouse (~10⁶ cells/ml) and then cultured on a 96-well plate at 100 μl/well. Finally, through a second screening by ELISA, HA-reactive clones were stocked. To prepare antibodies produced by these clones, cultured hybridomas were inoculated intraperitoneally into female BALB/c mice previously stimulated with pristane (Sigma) at 7 days prior to hybridoma inoculation. Antibodies were purified by protein G columns from the ascites fluids accumulated in hybridoma-inoculated mice.

In Vitro Viral Neutralization Assay—Viral neutralization by antibodies was tested *in vitro* by focus reduction neutralization test (FRNT) (10). Sera collected from immunized animals were treated with three volumes of receptor-destroying enzyme

(RDE) (RDE(II) "SEIKEN," Denka Seiken) for 16 h at 37 °C, and the enzyme was inactivated by incubation for 30 min at 56 °C. In the case of purified antibodies, this treatment was omitted. After adjusting to the appropriate concentrations, the RDE-treated sera or antibodies were mixed with an equal volume of MEM containing 2,000 focus-forming units of either influenza A/Hiroshima/52/2005 (H3N2), A/New Caledonia/20/1999 (H1N1), or A/duck/Czechoslovakia/1/1956 (H4N6) virus. After incubation for 1 h at 37 °C, 100 μl of the complexes were applied to 90% confluent Madin-Darby canine kidney cells in a 96-well plate. After incubation for 1 h at 37 °C, medium was changed to MEM containing 10% FBS, and incubation was continued overnight. Infected cells were visualized by an immunofluorescence assay as described below and counted. The changes in number of infected cells were represented as percentages calculated as $100 \times (N^- - N^+)/N^-$, where N^+ is the number of infected cells in the presence of antibody, and N^- is the average number of infected cells in the absence of antibody.

When antibody treatment was performed after viral adsorption, Madin-Darby canine kidney cells were previously incubated with virus in cold MEM without antibody for 1 h at 4 °C. After the removal of supernatant, cells were incubated with cold MEM containing the appropriate concentration of antibodies for 30 min at 4 °C followed by further incubation for 30 min at 37 °C. After changing the medium to MEM (plus 10% FBS), the assay was continued as described above.

Immunofluorescence Assay—Infected cells were treated with 4% (w/v) paraformaldehyde for 20 min and with 0.1% (v/v) Triton X-100 for 5 min at room temperature. Cells were then treated with antibody appropriately diluted in PBS for 1 h. After washing with PBS, cells were treated with secondary antibody labeled with Alexa Fluor 488 at 1:5,000 dilution for 1 h. After washing with PBS, cells were observed by fluorescence microscopy, and if necessary, cells with fluorescent focus were counted.

RESULTS

Design and Preparation of Modified EGFPs and mCherries Carrying Epitope-like Structure on Their Molecular Surfaces—The anti-parallel β-sheet region in HA focused on in the present study is composed of two separate sequences: residues 175–184 (upper) and 229–238 (lower). EGFP variants were first constructed by introducing substitutions at several positions that take part in its β-barrel scaffold. Corresponding to the side of the β-sheet in the epitope, two types of variants were possible: one type mimics the side facing the central axis of the HA trimer, and the other mimics the side facing laterally (Fig. 1, *A* and *B*). To design the former variant, named UL1, amino acids at EGFP residue positions 94, 96, 98, 100, 102, 179, 181, (183), 185, and 187 were substituted to Lys, Tyr, Trp, Val, His, Arg, Ser, (Tyr), Thr, and Val, respectively, which were originally located at residue positions 176, 178, 180, 182, 184, 229, 231, (233), 235, and 237 in HA1 of the major H3N2 strain. Upper region-only and lower region-only versions, named U1 and L1 respectively, were also constructed. Likewise, the latter variant, named UL2, was designed by introducing Asp-175, (Leu-177), Ile-179, Gly-181, His-183, Ile-230, Ile-232, Trp-234, Ile-236, and Lys-238 of HA1 onto EGFP at residue positions 177, (179),

181, 183, 185, 163, 165, 167, 169, and 171 (Fig. 1, *A* and *B*). Conformational similarity between the mutated region on EGFP and the corresponding region of the B-1 epitope was evaluated as the root mean square between Cα atoms (Table S2). No calculated root mean square value exceeded 2 Å. The relevance of these conformational gaps is discussed collectively with the results from immunization tests (see "Discussion"). Each EGFP variant was expressed in *E. coli* and purified. Fluorescence of the expressed protein was used as a helpful indicator of whether it has been folded successfully or not because the fluorophore formation of fluorescent proteins generally depends on folding accuracy of the entire molecule, including the β-barrel (11). Several variants were hardly expressed with the correct fluorescent conformations under culture at 37 °C, but by culturing at a lower temperature, such as 18 °C, every variant was expressed successfully. Every purified EGFP variant retained its fluorescence and distinct mobility after SDS-PAGE under non-boiling conditions (Fig. 1C). Equivalent variants of mCherry were prepared similarly to the EGFP variants.

Although the overall β-barrel scaffold of fluorescent proteins is nearly assured by their fluorescence (12, 13), we confirmed the structural relevance of EGFP UL1 and UL2 variants using far-UV CD spectra. Both variants demonstrated spectra similar to that of wild-type EGFP, indicating practically no change in secondary structure (supplemental Fig. S2).

Stability of EGFP Variants against Degradation and Denaturation—GFP and its derivatives are known to demonstrate high stability against protease digestion, detergent, and heat treatment (12), which are favorable for application as a scaffold for our immunogen carrier. We tested the protease resistance and thermostability of EGFP variants used here. Upon proK treatment, wild-type EGFP showed no significant decrease in fluorescence for up to 2 days at 37 °C. This finding indicates the maintenance of overall structure, because fluorescent proteins should generally lose their fluorescence by destruction of the β-barrel structure, even after the formation of their fluorophores (12, 13). Similarly, every variant used here maintained its fluorescence under proK treatment (Fig. 2, *A* and *B*). SDS-PAGE under non-boiling conditions revealed a fluorescent band for every proK-treated variant positioned slightly lower than that of variants with no proK treatment, whereas only proteolytic fragments appeared as a ladder when samples were boiled in SDS prior to electrophoresis (Fig. 2C). Upon heat treatment for 1 min at 80 °C, wild-type EGFP demonstrated no significant decrease in fluorescence (Fig. 2D). In the presence of 0.1% SDS, wild-type EGFP showed a sigmoidal decrease in fluorescence as temperature increased, with a denaturation temperature (T_d) of 62 °C (Fig. 2E). Each variant EGFP also demonstrated high thermostability comparable with wild-type EGFP in the absence of detergent (Fig. 2D). In the presence of 0.1% SDS, each variant EGFP demonstrated a distinct T_d value ranging from 58 to 76 °C (Fig. 2E). Similar to wild-type EGFP (14, 15), every EGFP variant showed a decrease in fluorescence at low pH. Wild-type and variants except UL2 showed 50% fluorescence at pH 6.0 (pH 6.4 for UL2) compared with the fluorescence at pH 7.2, but the change in fluorescence was fully reversible at values as low as pH 3.0 (data not shown). Collec-

A

EGFP	94	V	Q	E	R	T	I	F	F	K 102	179	L	A	D	H	Y	Q	Q	N	T 187
mCherry	97	K	W	E	R	V	M	N	F	E 105	179	D	A	E	V	K	T	T	Y	K 187
		↓		↓		↓		↓		↓		↓		↓		↓		↓		↓
UL1		K		Y		W		V		H		R		S		Y		T		V
HA1 residue#		176		178		180		182		184		229		231		233		235		237
		Upper-derived										Lower-derived								

EGFP	163	K	V	N	F	K	I	R	H	N 171	177	V	Q	L	A	D	H	Y	Q	Q 185
mCherry	163	K	G	E	I	K	Q	R	L	K 171	177	H	Y	D	A	E	V	K	T	T 185
		↓		↓		↓		↓		↓		↓		↓		↓		↓		↓
UL2		I		I		W		I		K		D		L		I		G		H
HA1 residue#		230		232		234		236		238		175		177		179		181		183
		Lower-derived										Upper-derived								

B

HA monomer
(viewed from central axis of the trimer)   EGFP UL1

HA monomer
(viewed from outside of the trimer)   EGFP UL2

C

EGFP   mCherry
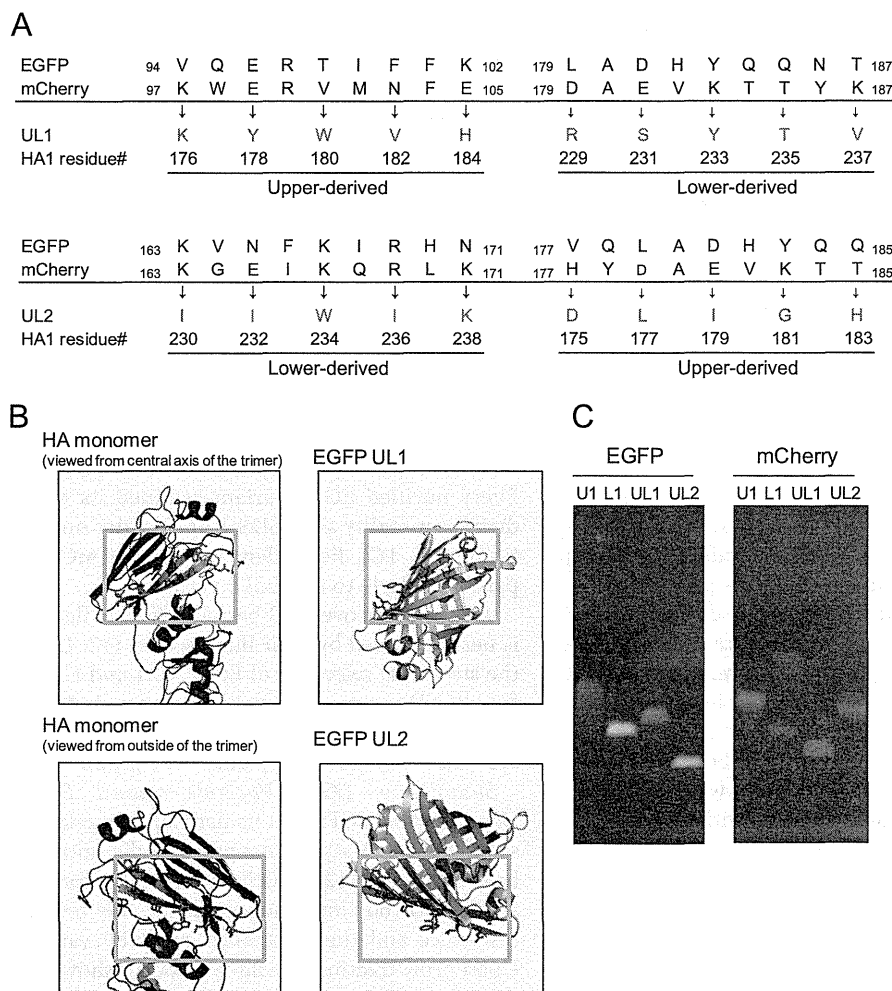
U1 L1 UL1 UL2   U1 L1 UL1 UL2

FIGURE 1. Modifications on EGFP and mCherry. *A*, schematic representation of EGFP and mCherry variants. *B, left panels*, monomeric HA structure (Protein Data Bank accession number 2VIU) with residues introduced to EGFP or mCherry indicated by *blue* (upper region) and *red* (lower region). *B, right panels*, EGFP carrying UL1 and UL2 mutations is illustrated by introducing modifications onto the EGFP structure (Protein Data Bank accession number 1EMA). The images were created with PyMOL (DeLano Scientific) and WinCoot (23). *C*, acrylamide gels after SDS-PAGE of EGFP or mCherry variants under non-boiling conditions. Images were taken under illumination on a 312-nm UV light box.

tively, we concluded that the EGFP variants used here were as stable as wild-type EGFP under physiological conditions and could be used equivalently for further examinations.

Reactivity and Viral Neutralization Activity of Sera from Modified EGFP-immunized Mice against H3-type HA—To test these EGFP variants as immunogens to induce production of anti-HA antibodies, we inoculated mice intraperitoneally with each variant as an emulsion with FCA. After a booster with the same immunogens, we collected serum from each mouse and tested the reactivity against either EGFP or HA by ELISA. As expected, every serum sample from wild-type and variant EGFP-immunized mice demonstrated major reactivity against EGFP (data not shown). We found sera from several mice immunized with EGFP U1 and UL1 variant that demonstrated significant reactivity with H3-type HA in vaccine solution (Fig. 3A). We also tested the *in vitro* viral neutralizing activity of each serum. FRNT (10) with the antisera revealed viral neutralizing activities almost parallel to immunoreactivities against HA (Fig. 3B). These results indicate that immunogenicity depends mainly on the inner side of the upper region.

Recognition of Cells Infected with H3N2-type Influenza Virus by Monoclonal Antibodies Raised against Modified EGFP—Of the mice immunized with either EGFP U1 or UL1 variant, two mice in each group whose sera showed positive reactivity with HA were finally boosted with the equivalent variant constructed on the mCherry scaffold. Hybridomas were prepared from their splenocytes. Culture supernatants of cell clones were screened by ELISA against either HA vaccine or wild-type EGFP. Although most clones demonstrated EGFP-specific reactivity as expected, several clones demonstrated HA-specific reactivity (Fig. 3C). HA-specific hybridoma clones were selectively isolated, and the monoclonal antibody secreted from each clone was purified. Reactivities of purified antibodies against HA were confirmed by ELISA (Fig. 3D). Unexpectedly, in the immunofluorescence assay, five of eight clones demonstrated very weak reactivity against Madin-Darby canine kidney cells infected with H3N2 virus (supplemental Fig. S3).

Viral Neutralization by Anti-variant-EGFP Monoclonal Antibody—We tested the *in vitro* viral neutralizing activity of the monoclonal antibodies isolated above against H3N2
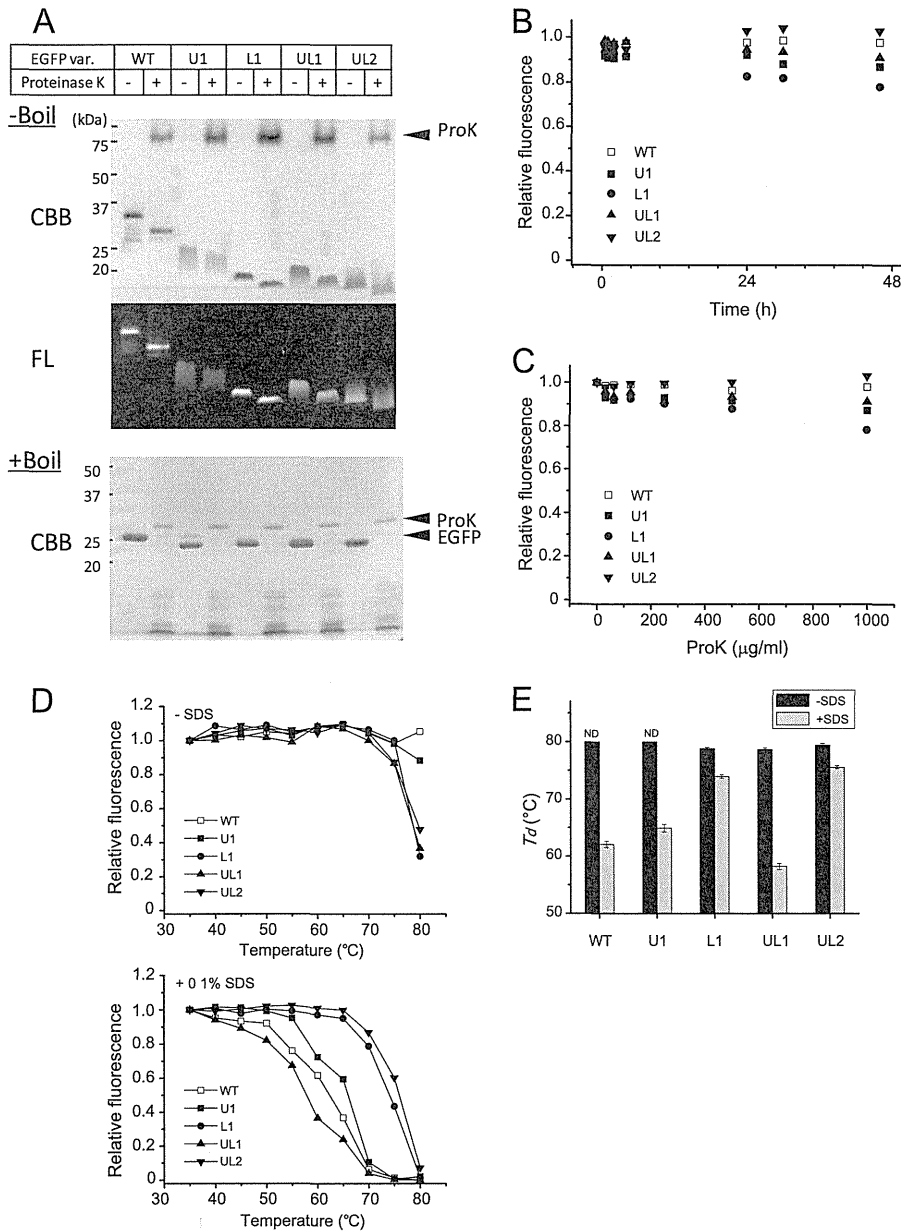
FIGURE 2. **Protease resistance and thermostability of EGFP and its variants.** *A,* EGFP and its variants (100 mM) were treated in the absence or presence of 1 mg/ml proK. After 48-h incubation at 37 °C, proteins were separated by SDS-PAGE with (*bottom panel*) or without (*top two panels*) boiling in sample buffer containing SDS before electrophoresis. In unboiled samples, a fluorescence image was also taken before Coomassie Brilliant Blue (*CBB*) staining. *B,* fluorescence of EGFP and its variants treated with or without proK as described in *A* was measured over time. *C,* EGFP and its variants were incubated with the indicated concentration of proK for 48 h at 37 °C, and fluorescence was measured. *D,* EGFP and its variants (100 nM) were incubated for 5 min at the indicated temperature in the presence (*bottom*) or absence (*top*) of 0.1% SDS, and fluorescence was measured. *E,* denaturation temperatures (T_d) calculated by fitting each denaturation curve with a sigmoid function are summarized. *Error bars,* S.E.; *ND,* not determined.

virus by FRNT. In the antibody concentration range tested here, one U1-derived clone and four UL1-derived clones demonstrated positive neutralizing activity. Notably, all FRNT-positive clones except 1E12 were nearly negative in the immunofluorescence assay, as described above (supplemental Fig. S3). Two FRNT-positive clones, 3H11 and 5E11, were further tested after the adsorption of virus (supplemental Fig. S4). In our experimental conditions, as many as 60% of virions would have already started to enter the cells during incubation at 4 °C without antibody. When B-1 antibody was

used as a positive control, ~40% of viruses at maximum were protected to infect after the adsorption onto cells. We found that both 3H11 and 5E11 also showed 40% protection at maximum after the viral adsorption. This observation may indicate that these antibodies recognize a state of HA after adsorption, in which the conformation may be changed to expose the epitope region (see "Discussion"). We also tested the viral neutralization of 3H11 and 5E11 against non-H3 strains H1N1 and H4N6. H1-HA was categorized as group 1, whereas H3-HA and H4-HA have been assigned to group 2
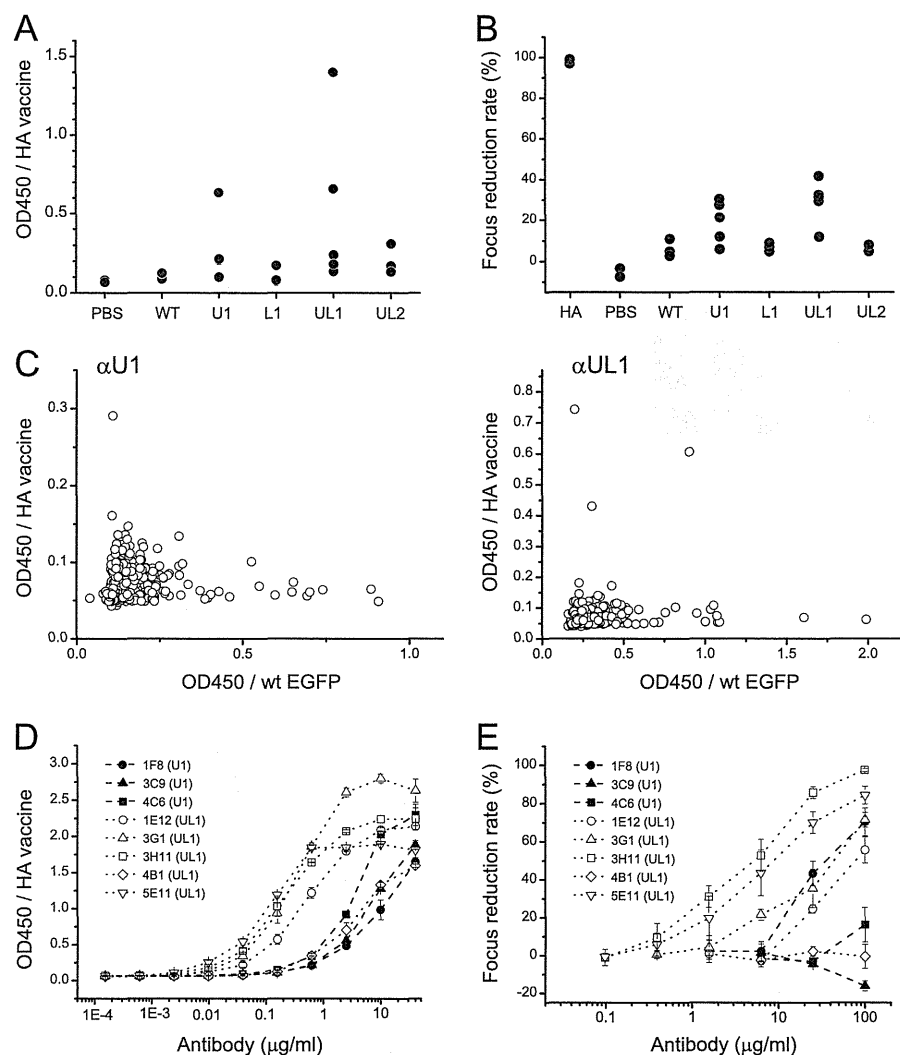
FIGURE 3. **Induction of anti-influenza neutralizing antibodies by modified EGFPs.** *A*, sera from mice immunized with EGFP or its variants were diluted 400-fold and tested by ELISA against HA vaccine. A PBS-immunized group was used as a negative control. n = 5 each for PBS, wild-type (*WT*), U1, UL1, and UL2; n = 3 for L1. *OD450*, optical density at 450 nm. *B*, viral neutralization by serum samples from mice immunized with each immunogen was tested by FRNT. An HA vaccine-immunized group (*HA*) was used as a positive control. RDE-treated serum was further diluted (ultimately 80-fold) and incubated with an equal volume of influenza H3N2 virus solution at 2,000 focus-forming units/ml. This complex was applied to Madin-Darby canine kidney cells, and infected cells were counted after immunofluorescent staining with an anti-NP antibody. Neutralization titer was estimated by focus reduction rate. *C*, culture supernatant of hybridomas prepared from splenocytes of two U1- or UL1-immunized mice whose serum demonstrated anti-HA reactivity were screened by ELISA against HA vaccine and wild-type EGFP. *D*, HA-reactive antibodies from each screened hybridoma clone were tested with ELISA against HA vaccine. *E*, using monoclonal antibodies raised against EGFP U1 and UL1 variants, viral neutralization was tested by FRNT. *Error bars*, S.E.

(16, 17). Residues corresponding to those we introduced on the UL1 variant are highly similar in H4-HA but not less similar in H1-HA (nine and six of 10 residues conserved, respectively). We found that neither 3H11 nor 5E11 demonstrated significant neutralization activity against H1N1 infection. Unexpectedly, H4N6 also showed no significant focus reduction by treatment with either 3H11 or 5E11. Because the differing residue between H3-HA and H4-HA is positioned in the upper region, this finding, together with the result shown in Fig. 3*B*, may also reflect the significance of the upper region in immunogenicity. Collectively, antibodies raised against the EGFP UL1 variant were able to neutralize virus in a serotype-dependent manner.

Acquisition of Immunity against Influenza Virus by Immunization with EGFP/mCherry Variants—We finally tested whether the mice inoculated with the designed immunogens acquired immunity against the influenza virus. Mice were first immunized with either 150 or 15 μg of wild type, U1, or UL1 variant of EGFP. Mice were boosted by equivalent variants of mCherry. These mice were then infected intranasally with reassortant mouse-adapted H3N2 virus. Approximately 6 days after infection, four of five mice in the positive control group that was immunized with seasonal influenza vaccine demonstrated recovery of body weight, with one mouse dead. Similar survival rates were observed in the EGFP/mCherry U1- and UL1-infected groups at high dosage (150 μg/body) (Fig. 4*A*). The effect
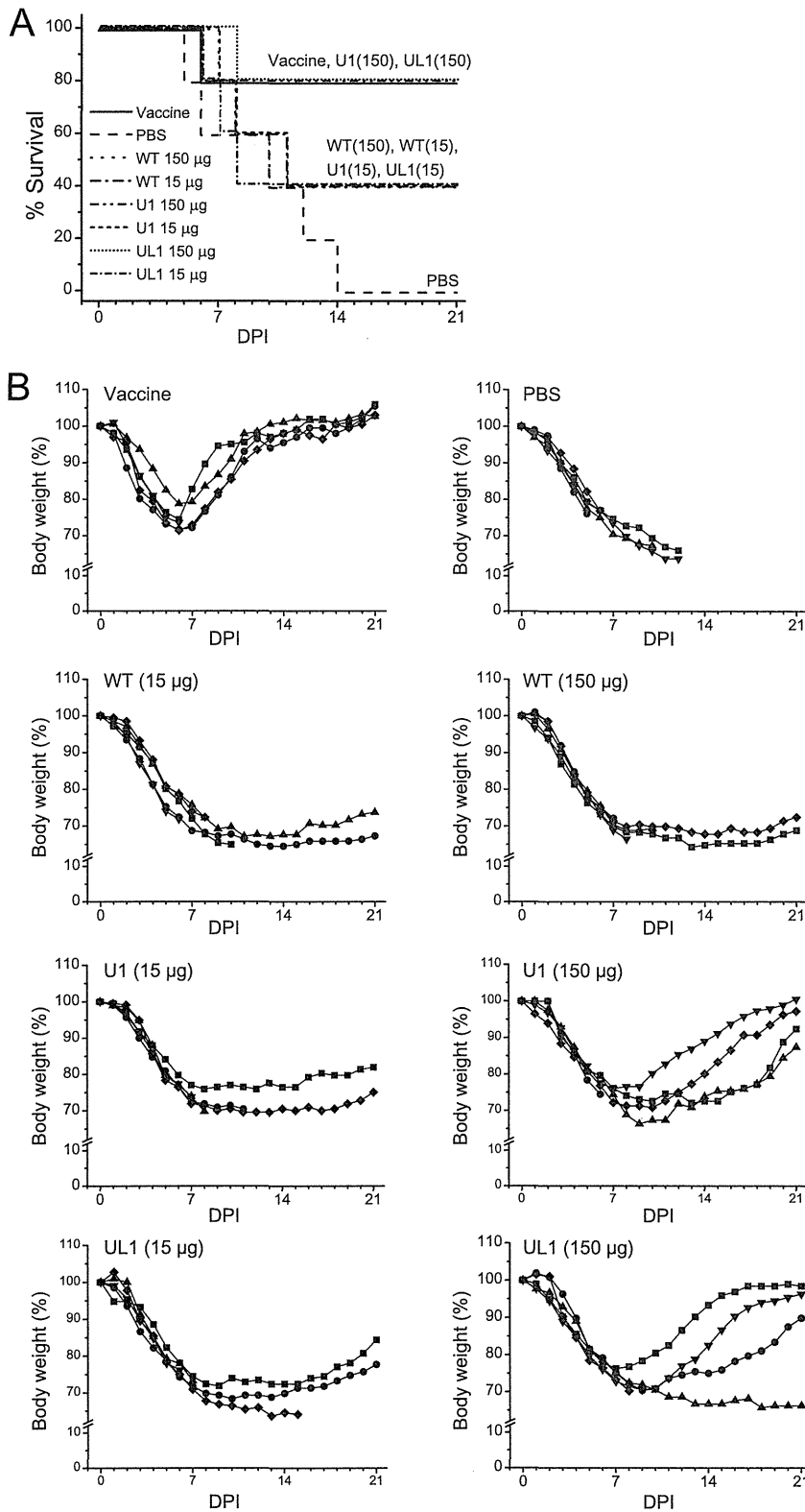
FIGURE 4. **Acquisition of anti-influenza immunity by modified EGFPs and mCherries.** Mice were immunized with either EGFP or its U1 or UL1 variant at 15 and 150 μg/body. After boosting with the equivalent variant of mCherry, mice were intranasally infected with influenza A H3N2 mouse-adapted virus. Mice immunized with seasonal vaccine were used as positive controls, and mice immunized with PBS mixed with adjuvant were used as negative controls. After infection, survival rate (*A*) and change in body weight (*B*) were recorded daily for 3 weeks. *DPI*, days postinfection.

of immunization with high dose U1 or UL1 variant was more apparent in recovery of body weight. In each group, one of five mice began to recover from 7 days after infection. Although the recovery rates were slower than those of the positive control group, four and three mice in the high dose U1- and UL1-infected groups, respectively, recovered body weight, whereas few signs of recovery were observed in either the PBS-immunized group or wild-type EGFP/mCherry-immunized groups within 3 weeks (Fig. 4B).

DISCUSSION

We have demonstrated a novel approach to induce immunity specifically against conformational epitopes characterized by β-sheet structure, proposing one form for the next generation of influenza vaccines. Although fluorescent proteins, such as those used here, may be unsuitable epitope carrier molecules for practical uses, they were sufficient to evaluate the validity of our strategy, and their fluorescence was quite helpful in confirming retention of the β-barrel structure in each variant, which is the most important point in this study. A similar approach can be found in recent investigations of amyloidosis, in which the β-sheet conformation of the pathogenic polypeptide is characteristic to its toxicity; several modified GFPs in which residues corresponding to the β-sheet region of the altered form of amyloid-β peptide were embedded in its surface β-barrel have been shown to interfere with the formation of toxic amyloid-β oligomer (18, 19). Conversely, our results suggest that proteins designed to carry a mimic of the surface structure of a toxic form of amyloid protein, such as amyloid-β or prion protein, may be used as vaccines against amyloidoses like Alzheimer disease and prion disease.

EGFP UL1 variant differs from wild-type EGFP by only nine residues. More strikingly, the U1 variant carrying just a five-residue difference was able to induce the production of anti-HA antibodies and anti-influenza immunity, although the isolated antibodies demonstrated weaker reactivity against HA and virus neutralization titers than those against the UL1 variant. The structural gaps represented as average root mean square values between the backbone Cα atoms of the mutated region of EGFP variants and that of the corresponding region of HA were ~1.4 Å for U1 and 1.7 Å for the UL1 variant. Our results indicate that such degrees of structural gap are allowable to induce primary immunity against a conformational epitope.

Because the target region focused on here seems mostly buried within the stable trimeric HA complex corresponding to the previously determined crystal structure models, questions remain concerning how it could induce antibodies, such as B-1, and how some antibodies raised against modified EGFPs, in which an epitope mimicking the structure of this region is embedded in the surface, could actually neutralize live virions. Using fluorescent cross-correlation spectroscopy, which enables the detection of interactions between elements by measuring the synchronism of fluorescent fluctuations (20, 21), we confirmed the H3-type-specific interaction between virion and B-1 antibody in a freely diffused state.[5] Antibodies against a nonapeptide derived from H3-HA spanning residues 98–106

(YPYDVPDYA), currently widely used as an epitope tag, namely the "HA tag," are known to react with intact trimeric HA despite the sequence also being located in a less accessible region in the crystal structure of HA trimer (14). One possible model for this phenomenon is the existence of a certain conformational mode of HA that exposes the inner side of the globular head domain, whereby B-1 (or a similar antibody) attacks such HA variants harbored on the viral surface, although they may be non-functional proteins produced by occasional misfolding. An alternative model is that the antibodies recognize HAs in a certain conformational state as they emerge at a stage of the viral life cycle during which the β-sheet (upper/lower) regions are exposed. Recall that the FRNT-positive antibody clones isolated here demonstrated nearly negative results against H3N2-infected cells in the immunofluorescence assay. This finding may indicate that these antibodies attack HA in a limited conformation. Our observation that 3H11 and 5E11 antibodies demonstrated viral neutralization even after viral adsorption onto the cell surface also supports this model (supplemental Fig. S4).

In this study, we could not obtain any antibodies with neutralization titers as high as that of B-1 (supplemental Fig. S4). In Western blotting analysis, B-1 demonstrated only weak reactivity against U1, L1, and UL1 variants (data not shown), probably because the upper/lower-like structure presented on the surface of EGFP does not cover enough of the B-1 epitope. Although this type of immunogen may not be sufficient to induce the production of strong neutralizing antibodies like B-1, it has the advantage of rapid production. Especially in the case of outbreak of a newly emerged viral strain that is resistant to seasonal vaccines available at the time, vaccines that can be produced instantly should be more helpful than conventional vaccines that require several months to be supplied (1). Recombinant immunogens produced according to the strategy proposed here require less effort for strain selection because they target a highly conserved region. Even in the case of an emergence of strains carrying mutations at the target region, updated immunogens can be produced quickly through a simple redesign and expression in an appropriate system. One of the most concerning current threats is the possible adaptation of highly pathogenic avian influenza A H5N1 virus into humans to cause serious pandemics (22). We have already confirmed that EGFP variants corresponding to residues from H5-HA as well as H1-HA can be prepared successfully. After steps of improvement, we expect this type of designed immunogen to be a highly valuable backup strategy for forthcoming pandemics.

REFERENCES

1. Gerdil, C. (2003) The annual production cycle for influenza vaccine. *Vaccine* **21**, 1776–1779
2. Novel Swine-Origin Influenza A (H1N1) Virus Investigation Team, Dawood, F. S., Jain, S., Finelli, L., Shaw, M. W., Lindstrom, S., Garten, R. J., Gubareva, L. V., Xu, X., Bridges, C. B., and Uyeki, T. M. (2009) Emergence of a novel swine-origin influenza A (H1N1) virus in humans. *N. Engl. J. Med.* **360**, 2605–2615
3. Bishop, J. F., Murnane, M. P., and Owen, R. (2009) Australia's winter with the 2009 pandemic influenza A (H1N1) virus. *N. Engl. J. Med.* **361**, 2591–2594
4. Kubota-Koketsu, R., Mizuta, H., Oshita, M., Ideno, S., Yunoki, M., Kuhara,

---

[5] Y. Inoue, F. Fujii, and K. Ikuta, unpublished data.

M., Yamamoto, N., Okuno, Y., and Ikuta, K. (2009) Broad neutralizing human monoclonal antibodies against influenza virus from vaccinated healthy donors. *Biochem. Biophys. Res. Commun.* **387,** 180–185

5. Yamashita, A., Kawashita, N., Kubota-Koketsu, R., Inoue, Y., Watanabe, Y., Ibrahim, M. S., Ideno, S., Yunoki, M., Okuno, Y., Takagi, T., Yasunaga, T., and Ikuta, K. (2010) Highly conserved sequences for human neutralization epitope on hemagglutinin of influenza A viruses H3N2, H1N1 and H5N1. Implication for human monoclonal antibody recognition. *Biochem. Biophys. Res. Commun.* **393,** 614–618

6. Ben-Yedidia, T., and Arnon, R. (2007) Epitope-based vaccine against influenza. *Expert Rev. Vaccines* **6,** 939–948

7. Staneková, Z., and Varečková, E. (2010) Conserved epitopes of influenza A virus inducing protective immunity and their prospects for universal vaccine development. *Virol. J.* **7,** 351

8. Shaner, N. C., Campbell, R. E., Steinbach, P. A., Giepmans, B. N., Palmer, A. E., and Tsien, R. Y. (2004) Improved monomeric red, orange, and yellow fluorescent proteins derived from *Discosoma* sp. red fluorescent protein. *Nat. Biotechnol.* **22,** 1567–1572

9. Okuno, Y., Isegawa, Y., Sasao, F., and Ueda, S. (1993) A common neutralizing epitope conserved between the hemagglutinins of influenza A virus H1 and H2 strains. *J. Virol.* **67,** 2552–2558

10. Okuno, Y., Tanaka, K., Baba, K., Maeda, A., Kunita, N., and Ueda, S. (1990) Rapid focus reduction neutralization test of influenza A and B viruses in microtiter system. *J. Clin. Microbiol.* **28,** 1308–1313

11. Cody, C. W., Prasher, D. C., Westler, W. M., Prendergast, F. G., and Ward, W. W. (1993) Chemical structure of the hexapeptide chromophore of the *Aequorea* green-fluorescent protein. *Biochemistry* **32,** 1212–1218

12. Bokman, S. H., and Ward, W. W. (1981) Renaturation of *Aequorea* green-fluorescent protein. *Biochem. Biophys. Res. Commun.* **101,** 1372–1380

13. Ward, W. W., and Bokman, S. H. (1982) Reversible denaturation of *Aequorea* green-fluorescent protein. Physical separation and characterization of the renatured protein. *Biochemistry* **21,** 4535–4540

14. Wilson, I. A., Niman, H. L., Houghten, R. A., Cherenson, A. R., Connolly, M. L., and Lerner, R. A. (1984) The structure of an antigenic determinant in a protein. *Cell* **37,** 767–778

15. Ward, W. W., Prentice, H. J., Roth, A. F., Cody, C. W., and Reeves, S. C. (1982) *Photochem. Photobiol.* **35,** 803–808

16. Nobusawa, E., Aoyama, T., Kato, H., Suzuki, Y., Tateno, Y., and Nakajima, K. (1991) Comparison of complete amino acid sequences and receptor-binding properties among 13 serotypes of hemagglutinins of influenza A viruses. *Virology* **182,** 475–485

17. Air, G. M. (1981) Sequence relationships among the hemagglutinin genes of 12 subtypes of influenza A virus. *Proc. Natl. Acad. Sci. U.S.A.* **78,** 7639–7643

18. Takahashi, T., Ohta, K., and Mihara, H. (2007) Embedding the amyloid β-peptide sequence in green fluorescent protein inhibits Aβ oligomerization. *Chembiochem* **8,** 985–988

19. Takahashi, T., Ohta, K., and Mihara, H. (2010) Rational design of amyloid β peptide-binding proteins. Pseudo-Aβ β-sheet surface presented in green fluorescent protein binds tightly and preferentially to structured Aβ. *Proteins* **78,** 336–347

20. Eigen, M., and Rigler, R. (1994) Sorting single molecules. Application to diagnostics and evolutionary biotechnology. *Proc. Natl. Acad. Sci. U.S.A.* **91,** 5740–5747

21. Kettling, U., Koltermann, A., Schwille, P., and Eigen, M. (1998) Real-time enzyme kinetics monitored by dual-color fluorescence cross-correlation spectroscopy. *Proc. Natl. Acad. Sci. U.S.A.* **95,** 1416–1420

22. Amendola, A., Ranghiero, A., Zanetti, A., and Pariani, E. (2011) Is avian influenza virus A (H5N1) a real threat to human health? *J. Prev. Med. Hyg.* **52,** 107–110

23. Emsley, P., and Cowtan, K. (2004) Coot. Model-building tools for molecular graphics. *Acta Crystallogr. D Biol. Crystallogr.* **60,** 2126–2132